THE FAILURE OF PRESSURIZED THIN-WALLED CYLINDERS

Thesis by

Ruben M. Gloria

In Partial Fulfillment of the Requirements

for the Degree of

Aeronautical Engineer

California Institute of Technology

Pasadena, California

1957

ACKNOWLEDGMENT

The author wishes to take this opportunity to express his appreciation to Dr. E. E. Sechler for his guidance; to Dr. M. L. Williams, and Dr. G. W. Housner; and to M. Lock and W. Christiansen for their collaboration during the research.

Acknowledgment is made to Messrs. C. A. Bartsch, M. E. Jessey, and M. J. Wood for their assistance in technical details and for their cooperation on all requests.

Thanks are extended to Misses H. Burrus and J. Maxwell for their preparation of the manuscript, and to Mrs. M. J. Wood for her preparation of drawings.

ABSTRACT

The object of this research was to find significant parameters in the failure of thin-walled internally pressurized cylinders. The following tests were made: (a) original crack length variation; (b) crack angle variation; (c) variation of velocity of penetration and (d) shape of a penetrating object; (e) cycling of internal pressure; and (f) change of loading media. The corresponding results were as follows: (a) the crack length parameter $\frac{l^2}{td}$ was found to bear importantly on the failing pressure of prepunctured cylinders; (b) an increase in failing pressure was achieved by changing the crack angle, originally parallel to the cylinder axis, to a perpendicular position; (c) explosive pressure level increased with decreased projectile velocity; (d) nondimensional explosive level increased with increased projectile sharpness, cylinder thickness and diameter; (e) pressure cycling tests revealed relatively fast crack growth during the first part of the life, followed by stabilization, and suceeded by another fast growth and failure; (f) a change from air to water as loading media made no effect on the static failing pressure of prepunctured cylinders.

The following tests are recommended: (a) determination of a parameter more generalized than $\frac{l^2}{td}$, involving cylinder length; (b) more crack angle tests to obtain a family of $\frac{P_f}{P_u}$ vs α curves for various crack lengths from which effective crack lengths may be obtained; (c) explosive level runs using higher velocity and true conical projectiles; (d) pressure cycling tests to find the effect of cycling stress level on crack propagation; and (e) crack propagation by vibration, using different loading media.

TABLE OF CONTENTS

LIST OF FIGURES

LIST OF TABLES

I. INTRODUCTION

Since flight is occurring at ever increasing altitudes, the problem of maintaining the structural integrity of the airplane fuselage as a pressure vessel becomes increasingly important. As a first approach, the fuselage may be represented by a pure monocoque structure; and for experimental purposes thin-walled internally pressurized cylinders may be used.

It was the purpose of this investigation to discover the important parameters governing the failure of such cylinders. Full scale tests have been conducted by the Royal Aircraft Establishment, Farnborough, the aircraft industry, and the National Advisory Committee for Aeronautics (Refs. 1 to 7) on critical crack lengths of fuselages under static pressure and crack propagation under pressure cycling. However, these large scale tests have dealt with specialized specimens and have been conducted mainly to establish fail-safe and safe-life structure.

Previous work by Sechler (Ref. 8) on thin, circular brass and aluminum membranes revealed that: (a) no failure will occur if puncturing is done 10-20 percent below ultimate failing pressure; (b) the margin of safety after puncture is increased by preloading to the highest possible pressure; (c) rate of crack propagation increases with the cycling pressure in a punctured specimen; and (d) crack propagation rate is increased by vibration of the membrane. It was suggested that similar tests be done on cylinders to supplement the membrane results.

The stress distribution in the walls of a simple cylinder is described in Appendix I. The notation used in this report is also explained.

II. SPECIMEN AND EQUIPMENT

A. Description of Specimen Used in Each Test:

In this sub-section, the number of specimen and the diameter and thickness of the cylinders for every series of tests are given. Not included are some ultimate pressure tests. Unless otherwise specified, the specimen were under internal pressure loading only.

1. Crack length variation tests:
   a. Eight 5"-0.003" cylinders with increasing crack length (Table I).
   b. Twelve 5"-0.001" cylinders with increasing crack length (Table II).
   c. Eighteen 3"-0.001" cylinders with increasing crack length (Table III).
2. Crack angle variation tests:
   a. Fourteen 5"-0.001" cylinders with 0.125" cracks at increasing angle (Table IV).
   b. Eight 5"-0.001" cylinders with 0.125" cracks at increasing angle (Table V).
3. Explosive level tests of unpunctured cylinders under penetration by projectiles (See Table VII):
   a. Several 3"-0.001", 4"-0.001", 5"-0.001", and 6"-0.001" cylinders under low velocity pellet penetration (Table VI A).
   b. Several 3"-0.001", 4"-0.001", 5"-0.001", and 6"-0.001" cylinders under high velocity pellet penetration (Table VI A).

c. Several 3"-0.003", 4"-0.003", 5"-0.003" and 6"-0.003" cylinders under high velocity pellet penetration (Table VI A).

d. Several 3"-0.001" and 5"-0.001" cylinders under low velocity dart penetration (Table VI B).

e. Several 3"-0.001", 4"-0.001", 5"-0.001" and 6"-0.001" cylinders under high velocity dart penetration (Table VI B).

f. Several 3"-0.003", 4"-0.003", 5"-0.003" and 6"-0.003" cylinders under high velocity dart penetration (Table VI B).

4. Pressure cycling tests:

a. One 3"-0.001" cylinder with initial crack length of 0.260", cycled from 0 - 14 psig (Table XII).

b. One 3"-0.001" cylinder with initial crack length of 0.310" cycled from 0 - 14 psig (Table XIII).

c. One 5"-0.001" cylinder with initial crack length of 0.200" cycled from 0 - 12 psig (Table XIV).

d. One 5"-0.003" cylinder with initial crack length of 0.240" cycled from 0 - 50 psig (Table XV).

5. Media comparison tests for cylinders with 0.125" initial crack (Table XVI):

a. Three 3"-0.004" cylinders under water pressure.

b. Three 3"-0.004" cylinders under air pressure.

c. Three 3"-0.003" cylinders under water pressure.

d. Three 3"-0.003" cylinders under air pressure.

e. Three 4"-0.004" cylinders under water pressure.

f. Three 4"-0.004" cylinders under air pressure.

g. Three 3"-0.002" cylinders under water pressure.

h. Three 3"-0.002" cylinders under air pressure.

i. Five 6"-0.004" cylinders under water pressure.

j. Two 6"-0.004" cylinders under air pressure.

k. Three 4"-0.002" cylinders under water pressure.

l. Three 4"-0.002" cylinders under air pressure.

m. Three 6"-0.003" cylinders under water pressure.

n. Three 6"-0.003" cylinders under air pressure.

o. Three 5"-0.002" cylinders under water pressure.

p. Three 5"-0.002" cylinders under air pressure.

q. Four 3"-0.001" cylinders under water pressure.

r. Three 3"-0.001" cylinders under air pressure.

s. Three 6"-0.002" cylinders under water pressure.

t. Three 6"-0.002" cylinders under air pressure.

u. Three 5"-0.001" cylinders under water pressure.

v. Three 5"-0.001" cylinders under air pressure.

w. Three 6"-0.001" cylinders under water pressure.

x. Three 6"-0.001" cylinders under air pressure.

B. Description and Assembly of Cylinders:

The cylinders (Fig. 1) were all of the same length, six and one half inches externally with five and one half inches working length (minus the ends). Diameters were 3, 4, 5, and 6 inches and thicknesses were 0.001, 0.002, 0.003, 0.004, and 0.005 inches. Brass was used as material because it made assembly an easier task. Attempts were made to assemble aluminum cylinders without successful results.

Assembly of cylinders was the most serious bottleneck during the research. To assure air- and water- tightness under pressure, the cylinders were soldered together; first, by lapping brass sheet stock around a cylindrical form, and then soldering this "tube" to the circular brass ends with the aid of a hot plate. The grain of the material thus ran circumferentially and the ends may be considered to have been infinitely rigid. The brass sheet stock was 6 inches wide and came in 100 inch and 100 foot lengths. Thicknesses varied from 0.001 to 0.005 inch. 100 inch lengths were used in media comparison tests.

The ends had 2 inch diameter holes to facilitate assembly. Into these holes went threaded collars to which a pressure supply or gage was connected via quick-disconnect coupling.

The assembled cylinder was mounted in a frame such that it rested freely on its inlet and outlet piping, thus allowing freedom in axial translation, in bending, and in twist. The test pressures were such that forces therefrom greatly overshadowed body forces due to the weight of the cylinder. The specimens were subjected to internal pressure only, no other loadings were applied (except during the explosive level tests, when the specimens were subjected to impact from the projectiles).

C. Pressurization:

Air and water were used as internal loading media, and in all test runs the cylinders were immersed within either medium. Pressure was introduced into one end of the cylinder (via a water valve or air pressure regulator) and a gage was connected to the other end.

House air and water pressure were sufficient for a great majority of the tests, but for higher pressures a nitrogen bottle or a water pump and accumulator were employed.

During the pressure cycling tests (Fig. 2) only water was used. Pressure was cycled from almost zero to maximum by rotation of an inlet on-off valve which was driven by a geared-down electric motor. Pressure was relieved through the crack during the "off" position of the valve. Overshooting of maximum pressure was prevented by a preset pop-off valve which bled water between the rotating inlet valve and cylinder. A Veeder counter connected directly to the rotating valve was used to determine the number of cycles.

D. Explosive level test equipment:

The description of equipment used during these tests has been integrated into TEST PROCEDURE (p. 9, see Figures 3 and 4).

III. TEST PROCEDURE

A. Crack Manufacture:

In all but the explosive level tests, initial knife-edge cracks were located centrally between the ends and opposite the axial seam of the cylinders in order to escape end and seam effects as much as possible. The cracks were made with a square-tipped knife having a 0.015" x 0.125" cross section. Longer cracks were made by repeated puncture. Crack lengths were measured to .001 inch with a Bell and Howell pocket comparator. During pressure cycling runs a 6 volt lamp was placed inside the cylinder to facilitate reading of progressing crack lengths.

In all but the explosive level tests, punctures were made on the flat brass sheet before assembly of the cylinders so that close control could be achieved. The cylinders were assembled so that the crack lips protruded outside to prevent closure during efflux, subsequent premature pressure buildup and failure.

B. Ultimate Failing Pressure:

Failing pressures were to be normalized against ultimate (no crack) pressure, therefore during every test run, randomly chosen cylinders were failed at ultimate pressure. Since tensile tests revealed that batch materials differed greatly in strength, ultimate pressure tests were made as soon as a new batch was used. In order to save time and to conserve material within a batch, a few ultimate pressures for different diameters were scaled from results for one diameter. The validity of this method has been borne out by actual testing.

The majority of ultimate (no hole) failures have occurred at the axial seam due to soldering effects. However, the results of some failures away from the seam have indicated that the failures at the axial seam were very close to true ultimate.

All ultimate failures were due to internal pressure alone.

C. Length Variation Tests:

It was desired to find the influence of crack length on failing pressure. Variations in crack length were made and failing pressures were recorded. Cracks were aligned parallel to the cylinder axis. Up to 0.700 inch cracks (13 per cent working length) were made. The following diameter-thickness combinations were used: 5"-0.001", 5"-0.003", and 3"-0.001". Water was used as the loading media since this did not alter results and repeated air failure was found to be irritating to the operators and to others in the building.

D. Crack Angle Variation Tests:

Failing pressures were recorded against crack angles which were measured from an axial line; thus a zero degree crack would be a typical crack used in the length variation tests above. A 90^{o} crack would run perpendicular to the axis, with the grain, and in the direction of maximum principal (hoop) stress. Two runs were made using 5"-0.001" cylinders with 0.125" long cracks each. Water was used as loading media.

E. Explosive Level Tests:

In this series of tests, projectiles were sent through air-filled cylinders to determine the critical pressure above which explosion would occur. Two kinds of projectiles were used (Fig. 3) i.e. relatively flat nosed pellets and darts. Notice that the darts were not

The majority of ultimate (no hole) failures have occurred at the axial seam due to soldering effects. However, the results of some failures away from the seam have indicated that the failures at the axial seam were very close to true ultimate.

All ultimate failures were due to internal pressure alone.

C. Length Variation Tests:

It was desired to find the influence of crack length on failing pressure. Variations in crack length were made and failing pressures were recorded. Cracks were aligned parallel to the cylinder axis. Up to 0.700 inch cracks (13 per cent working length) were made. The following diameter-thickness combinations were used: 5"-0.001", 5"-0.003", and 3"-0.001". Water was used as the loading media since this did not alter results and repeated air failure was found to be irritating to the operators and to others in the building.

D. Crack Angle Variation Tests:

Failing pressures were recorded against crack angles which were measured from an axial line; thus a zero degree crack would be a typical crack used in the length variation tests above. A 90° crack would run perpendicular to the axis, with the grain, and in the direction of maximum principal (hoop) stress. Two runs were made using 5"-0.001" cylinders with 0.125" long cracks each. Water was used as loading media.

E. Explosive Level Tests:

In this series of tests, projectiles were sent through air-filled cylinders to determine the critical pressure above which explosion would occur. Two kinds of projectiles were used (Fig. 3) i.e. relatively flat nosed pellets and darts. Notice that the darts were not

true cone-shaped projectiles. With the exception of low velocity dart tests, the projectiles went through both sides of the cylinders, along a diameter.

High velocity punctures were made by shooting darts and pellets from a 22 caliber Crossman Model 220 airgun (Fig. 3). Distance between muzzle and cylinder was approximately 5 feet, and 10 pumps were used. Projectile velocity at this distance was determined with the aid of an electronic counter and triggering circuit. The projectile broke two 0.001" brass strips whereupon "start" and "stop" pulses were sent to the counter. Dividing the distance between the strips by the time to traverse (taken from the counter) produced average velocities of 315 fps for pellets and 250 fps for darts (Table VII). In spite of the difference in velocities, the kinetic energies of pellets and darts were practically equal (Appendix IV).

Low velocity pellet punctures were made with a pendulum arrangement shown in Figure 4. The operator held the weight up with a string, letting it down until the pellet came as close as possible to the cylinder, whereupon he let go. The pellet sting was long enough to go through both sides of the widest cylinder. Again, the line of puncture went through a diameter, and away from the seam as much as possible. Low velocity dart tests involved manual puncture with a sharp prong through one side.

High velocity dart and pellet runs were made on all diameters, 0.001" and 0.003" thick. Low velocity pellet runs were made on all diameters 0.001" thick. Low velocity dart runs were made on 1" and 3" diameters 0.001" thick. There were no low velocity tests made on 0.003" thick cylinders.

F. Pressure Cycling Tests:

Prepunctured cylinders were subjected to pressure fluctuating from zero to maximum cycling pressure and crack length was measured at intervals during the life of the specimen. Water was used as the loading media because relatively fast cycling rates could be achieved with it (due to its incompressibility) and time was of the essence. Since pressure was relieved through the crack during the "off" position of the inlet valve the cycling rate was limited by crack size. It is suggested that faster cycling rates may be achieved by using synchronized rotating inlet and outlet valves (mounted on the same shaft) along with larger lines and couplings (one half inch pipe was used).

5"-0.001", 5"-0.003", and 3"-0.001" cylinders were cycled to failure.

G. Media Comparison:

Since questions have been raised as to the validity of large-scale underwater tests, an extensive series of tests was carried out to find the difference between failing pressures of cylinders with 0.125" prepunctured cracks under air and water pressure. Cylinder diameters in this test ranged from 3" to 6" and thicknesses ranged from 0.001" to 0.005".

Media comparison took place within the same batch since (it was discovered by tensile tests) there was an appreciable difference of strength between batches. These tensile tests consisted in breaking 1" wide by 3" long strips in a tensile test machine. Thicknesses were taken from an average of two or three readings with a micrometer.

IV. RESULTS

In the presentation of results, failing pressures are normalized against ultimate (no hole) failing pressure. The purpose of this is to eliminate the effect of cylinder dimensions and to present a truer picture of relative strength between cylinder configurations.

A. Crack Length Variation:

Failing pressures normalized against ultimate failing pressure (Tables I to III) are plotted against crack length for 5"-0.001", 5"-0.003", and 3"-0.001" cylinders in Figure 5. A common curve is achieved by plotting pressures against crack length parameter $\frac{l^2}{td}$ in Figure 6. The crack propagation at failure was very rapid in all cases, and in the majority of failures the cracks extended to the ends, following a line normal to the hoop stress.

B. Crack Angle Variation:

From Figure 7 and Tables IV and V it is seen that failing pressures increase with increasing crack angle. The manner of failure was rapid, the crack following a line normal to the hoop stress.

A few tests with longer cracks indicated greater failing pressure variation with change of angle.

C. Explosive Level:

Actual values of explosive level went down with increased diameter (Fig. 8). This might be expected since ultimate pressures vary inversely with diameter. However, there was an upward trend of normalized explosive level with increased diameter (Fig. 9) with the exception of low velocity pellet tests.

Low velocity tests produced higher explosive levels than high velocity runs. Use of thicker material also raised the normalized explosive level. The same result was achieved by using sharper projectiles, although the difference between normalized pellet and dart levels was slight.

Among a few low velocity pellet tests the pellet did not penetrate the cylinder and left a dimple on the specimen, indicating a large amount of plastic deformation. Examination of high velocity pellet punctures revealed that the crack started at the sharply outlined circular pellet impression, where deformation was greatest. The angle of crack propagation during failure was quite random, not necessarily following an axial line. The boundary between leakage and explosive failure was sharp.

Energy calculations (Appendix II) revealed an upward trend in strain energy density and available air energy at critical pressure with increased diameter (Figs. 12 to 14, Tables IX to XI). The low velocity pellet results were an exception. Critical air energy for 0.003" thick cylinders was about 10 times greater than that for 0.001" thick cylinders.

Preliminary tests made by firing pellets at water filled cylinders broke the specimen at zero internal pressure due to the relatively high dynamic loadings.

D. Pressure Cycling:

Over twenty specimenswere cycled to failure however only four representative results are presented here because of the large amount of data scatter. The curves (Figs. 15 to 18, Tables XII to

XV) have one thing in common; namely a sharp increase in crack length at the outset, followed by relative stabilization, finally another sharp increase of crack growth and failure. Failure was "instantaneous".

A few trial runs with rotated cracks revealed the same type of failure as zero degree cracks - the cracks propagating along an axial line.

E. Media Comparison:

From Table XVI it is seen that there is no difference between air and water as loading media for static failure. Notice the difference in failing stresses between the different batches.

Weibull (Ref. 10), however, has noticed an appreciable difference in life between dry and kerosene dipped notched aluminum plate fatigue specimens.

V. CONCLUSIONS

A. Crack Length Variation:

The parameter $\frac{l^2}{td}$ is significant with regard to failing pressure for specimen having the same material and cylinder length.

B. Crack Angle Variation:

Static failing pressure increases with increasing crack angle, measured from an axial line.

C. Explosive Level:

Apparently the cylinder absorbs more dynamic energy during high velocity puncture than during low velocity puncture, hence the explosive level for high velocity puncture was lower (Fig. 8).

A sharply pointed projectile imparts less impact than a blunt one, therefore, the normalized explosive pressure level increased with increasing sharpness (Fig. 9).

The rise in normalized explosive levels with increased diameter and thickness (Fig. 9) may be explained by greater shock absorbing qualities of larger and thicker cylinders due to increased bulk.

The exception to the above is the low velocity pellet result. The fact that the strain energy densities (Fig. 13) at the critical pressures did not increase with diameter indicates that the added strain due to very low velocity penetration with blunt objects is spread out over a large portion of the cylinder. The cylinder may thus be treated as a static case subjected to point load. Whereas with sharp punctures, the resistance to penetration is restricted more to the material in the vicinity of the projectile.

D. Pressure Cycling:

Notched material under 2:1 biaxial cyclic tension behaves in similar fashion as it would under uniaxial cyclic tension. Both exhibit fast initial crack growth, followed by crack stabilization and fast growth to failure.

E. Media Comparison:

There is no difference between water and air as loading media for static failing pressure.

VI. RECOMMENDATIONS

A. Crack Length Variation:

Crack length variation tests involving cylinders of different lengths should be conducted to determine a parameter more generalized than $\frac{l^2}{td}$, which may involve cylinder length.

B. Crack Angle Variation:

Since static failure propagates along axial lines, it would be of interest to find "effective axial lengths" of rotated cracks. These would be axially oriented cracks having the same failing pressures as longer but rotated cracks. This may be used as a measure of strength for rotated cracks. (See Appendix III)

C. Explosive Level:

It follows from the velocity tests that the cylinder can absorb only a maximum of dynamic energy, therefore there must exist a minimum or limiting explosive level at higher velocity puncture. Tests should be done to bear this out.

Additional tests should be run with true conical shaped darts and knife-edged projectiles to determine if an upper limit of explosive pressure level exists.

A verification of normalized low velocity explosive pressure level results should be carried out by using thicker specimens.

D. Pressure Cycling:

More tests should be carried out to find the effect of cycling level on the crack propagation rate. It is recommended that these be carried out on thicker material since less data scatter was obtained from 0.003" thick cylinders.

E. Media Comparison:

Media comparison should be extended to vibration tests and/or cyclic loading.

REFERENCES

1. Walker, P. B.: Static Strength Tests of a Comet I Pressure Cabin. Structures Report No. 196, Royal Aircraft Establishment, Farnborough, (December 1955).

2. Inouye, H.: Test Progress Reports on Crack Propagation and Pressure Test of Full Scale 707 Fuselage Panel. Report No. T-29439, Boeing Airplane Company, Seattle, (October 1955 to April 1956). (Unpublished)

3. Ostergren, R. L.: Crack Propagation Due to Combining Torsion and Internal Pressure in a Fuselage Structure. Coordination Sheet No. SU-717-B-175, Boeing Airplane Company, Seattle, (April 1956). (Unpublished)

4. Structural Problems Associated with Vibration and Pressurization (C-133A Aircraft). Report No. LB-25051, Douglas Aircraft Company, Long Beach, (June 1956).

5. Gurin, P. J.: Window Panel Pressure Tests. Report No. 10,588, Lockheed Aircraft Corporation, Burbank, (May 1955).

6. EnEarl, R. O.: Pressure Repeated Load and Fail-Safe Tests of Fuselage Panel Structures. Report No. 10,593, Lockheed Aircraft Corporation, Burbank, (October 1955).

7. Dow, N. F. and Peters, R. W.: Preliminary Investigation of the Failure of Pressurized Stiffened Cylinders. NACA RM L55D15b, (May 1955).

8. Sechler, E. E.: Puncturing of Thin Walled Pressure Vessels and Crack Propagation. Progress Report No. 2, California Institute of Technology, (December 1954). (Unpublished)

9. Walker, P. B.: Destructive Energy in Aircraft Pressure Cabins. The Journal of the Royal Aeronautical Society, p. 235, Vol. 54, (1950).

10. Weibull, W.: The Propagation of Fatigue Cracks in Light-Alloy Plates. SAAB TN 25, (1954).

11. Paris, P. C.: Bibliography of Fracture Propagation Mechanics, Boeing Airplane Company, Seattle, (May 1956). (Unpublished)

12. Kies, J. A.: The Resistance of Materials to Fracture Propagation and Gunfire Damage. NRL Memorandum Report 594, (May 1956).

13. Hogan, M. B.: A Survey of the Literature Pertaining to Stress Distribution in the Vicinity of a Hole and the Design of Pressure Vessels. Bulletin Univ. of Utah, No. 48, Vol. 41, No. 2, (1950).

14. Williams, M. L.: On the Stress Distribution at the Base of a Stationary Crack. Presented at the Annual Meeting of the American Society of Mechanical Engineers, Paper No. 56-A-16, (Nov. 1956).

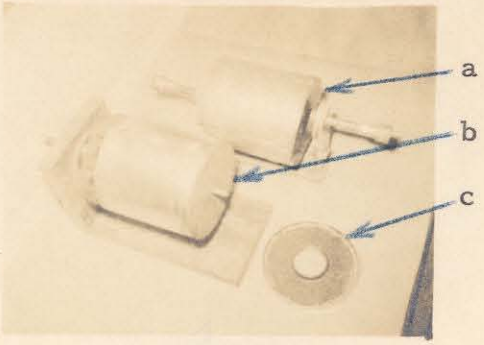

Fig. 1 Cylinder and Mounting Frame

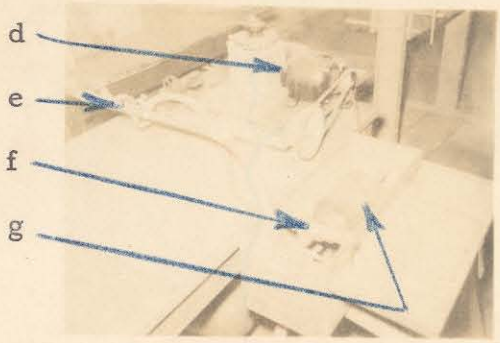

Fig. 2 Pressure Cycling Apparatus

a - Cylinder mounted on frame

b - Sheet lapping form

c - Cylinder end

d - Electric motor

e - Rotating "on" - "off" water valve

f - Pop-off valve

g - Cylinder under cycling pressure

h - Pellets

i - Darts

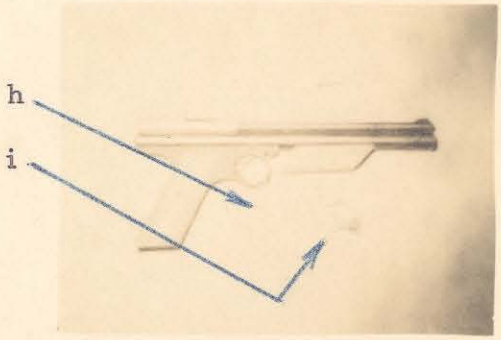

Fig. 3 High Velocity Explosive Level Equipment

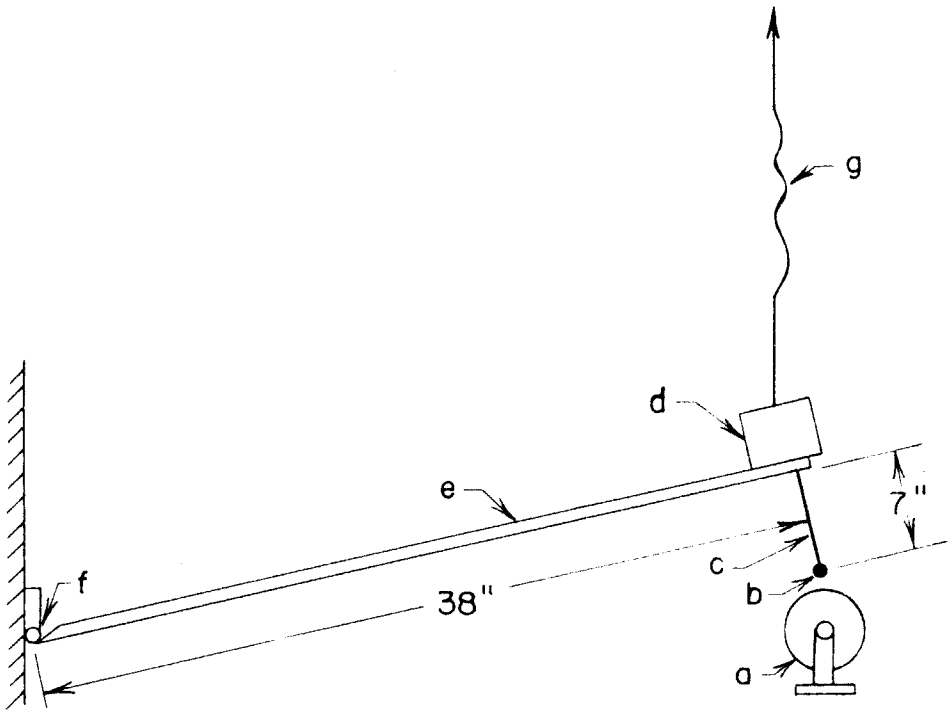

a Cylinder

b Pellet

c Pellet Sting

d 7 Lb. Weight

e Pendulum arm

f Hinge

g String (To Operator)

FIG. 4 - LOW VELOCITY EXPLOSIVE LEVEL SET UP

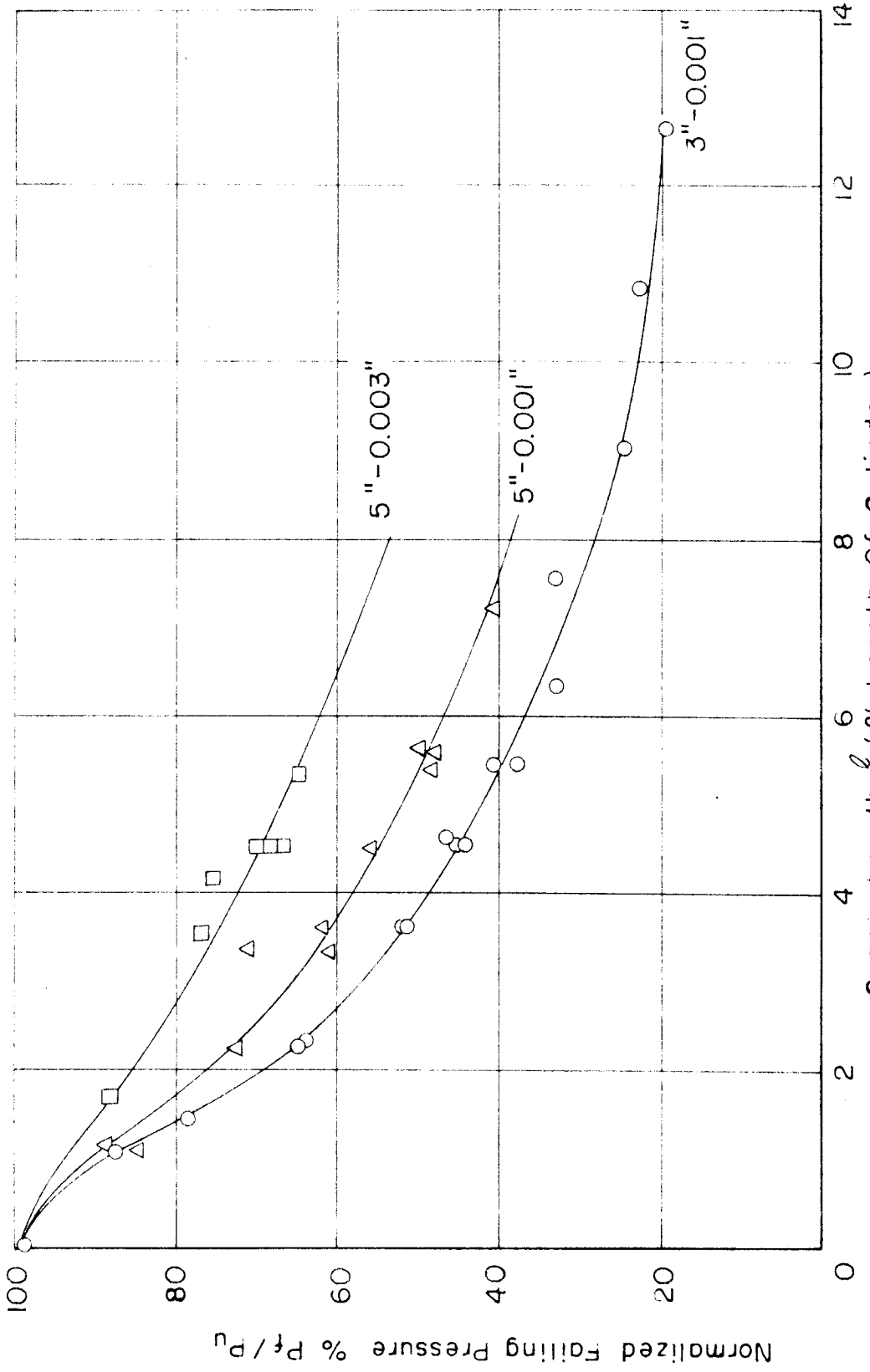

FIG. 5 — NORMALIZED FAILING LEVEL — CRACK LENGTH

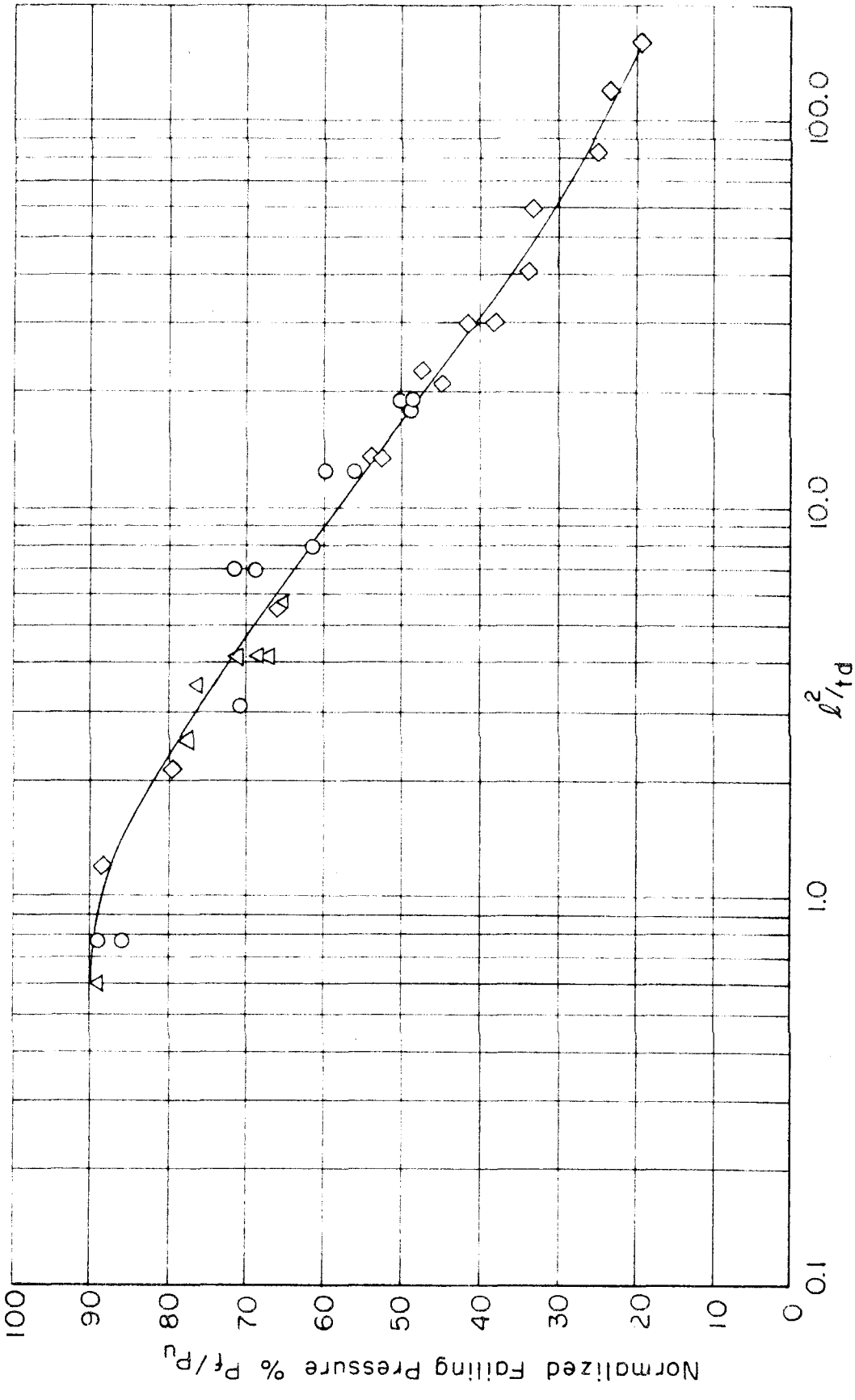

FIG. 6 — NORMALIZED FAILING LEVEL — $\frac{\ell^2}{t_d}$

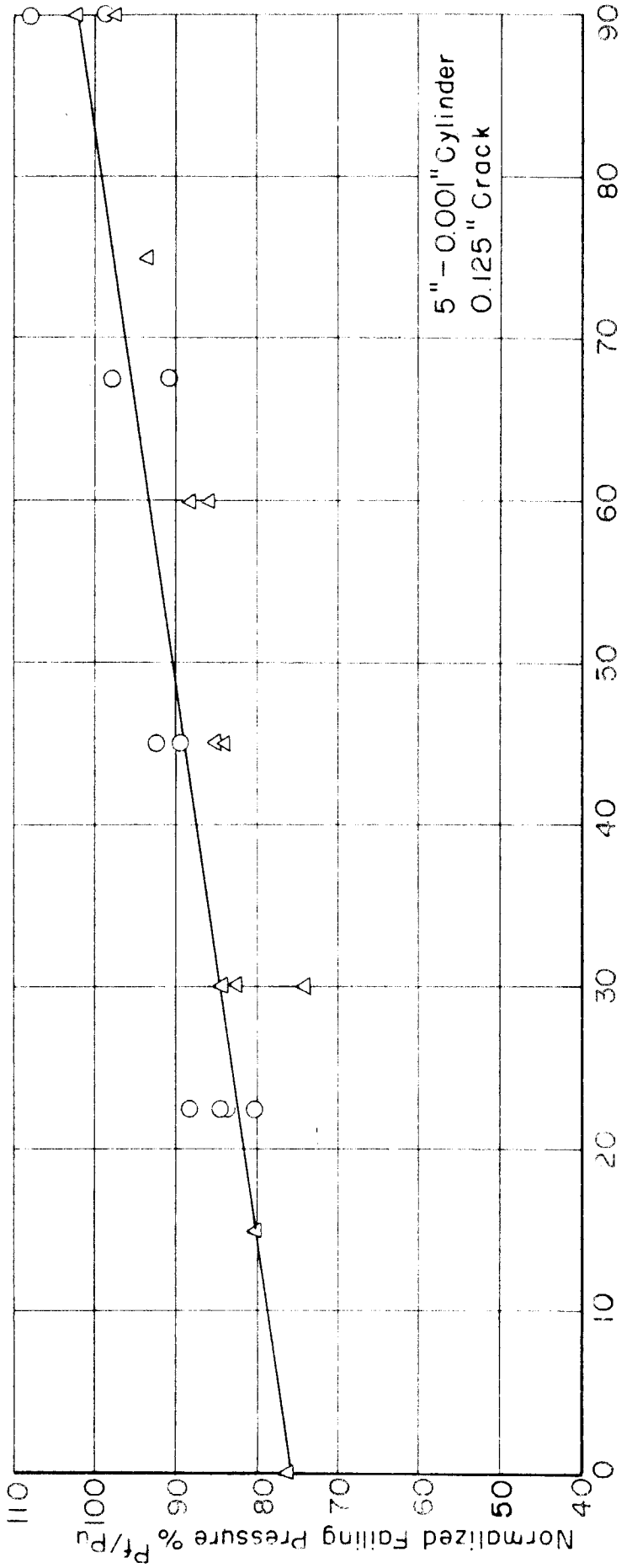

FIG. 7– NORMALIZED FAILING LEVEL – CRACK ANGLE

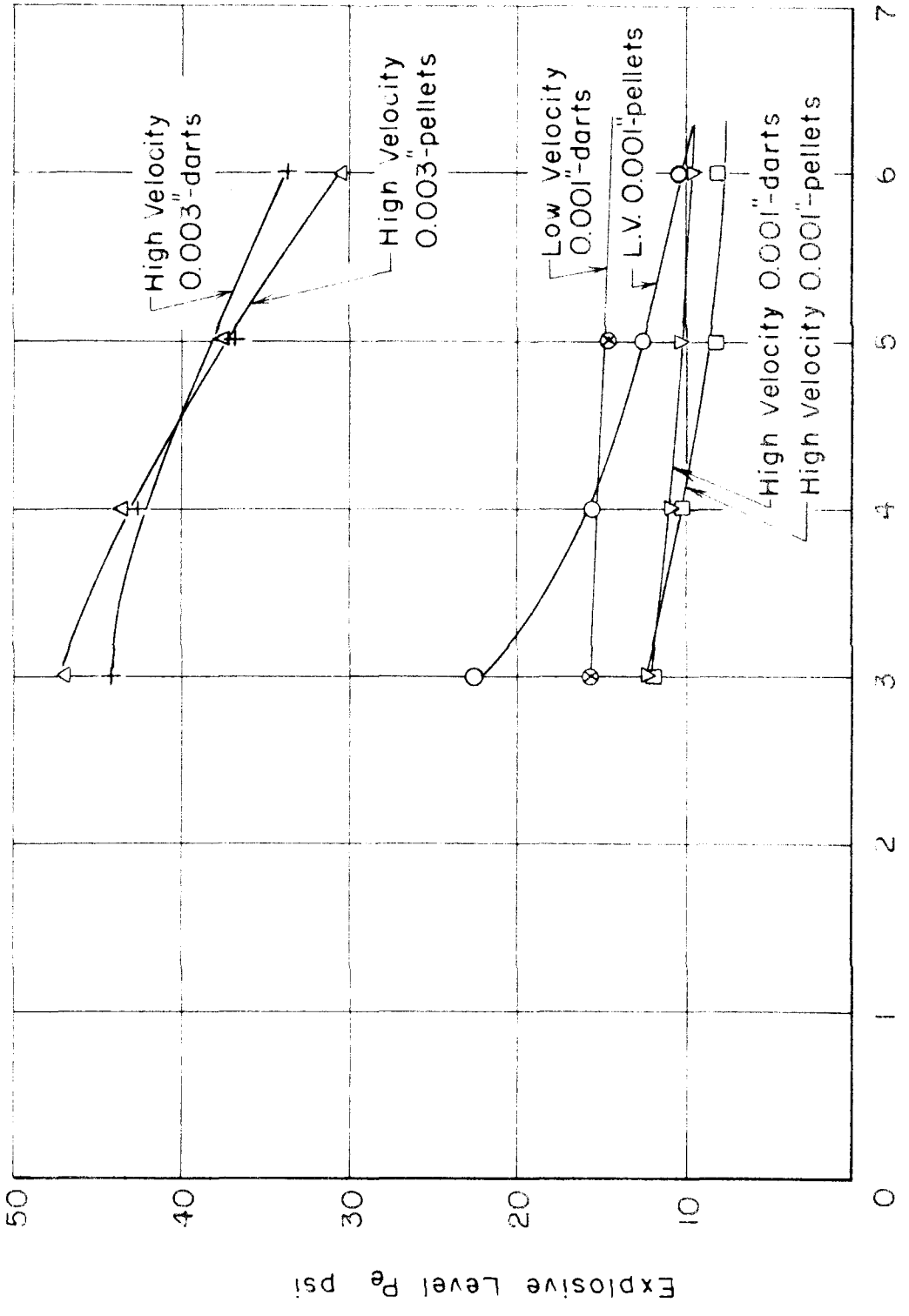

FIG. 8 - EXPLOSIVE LEVEL CURVES

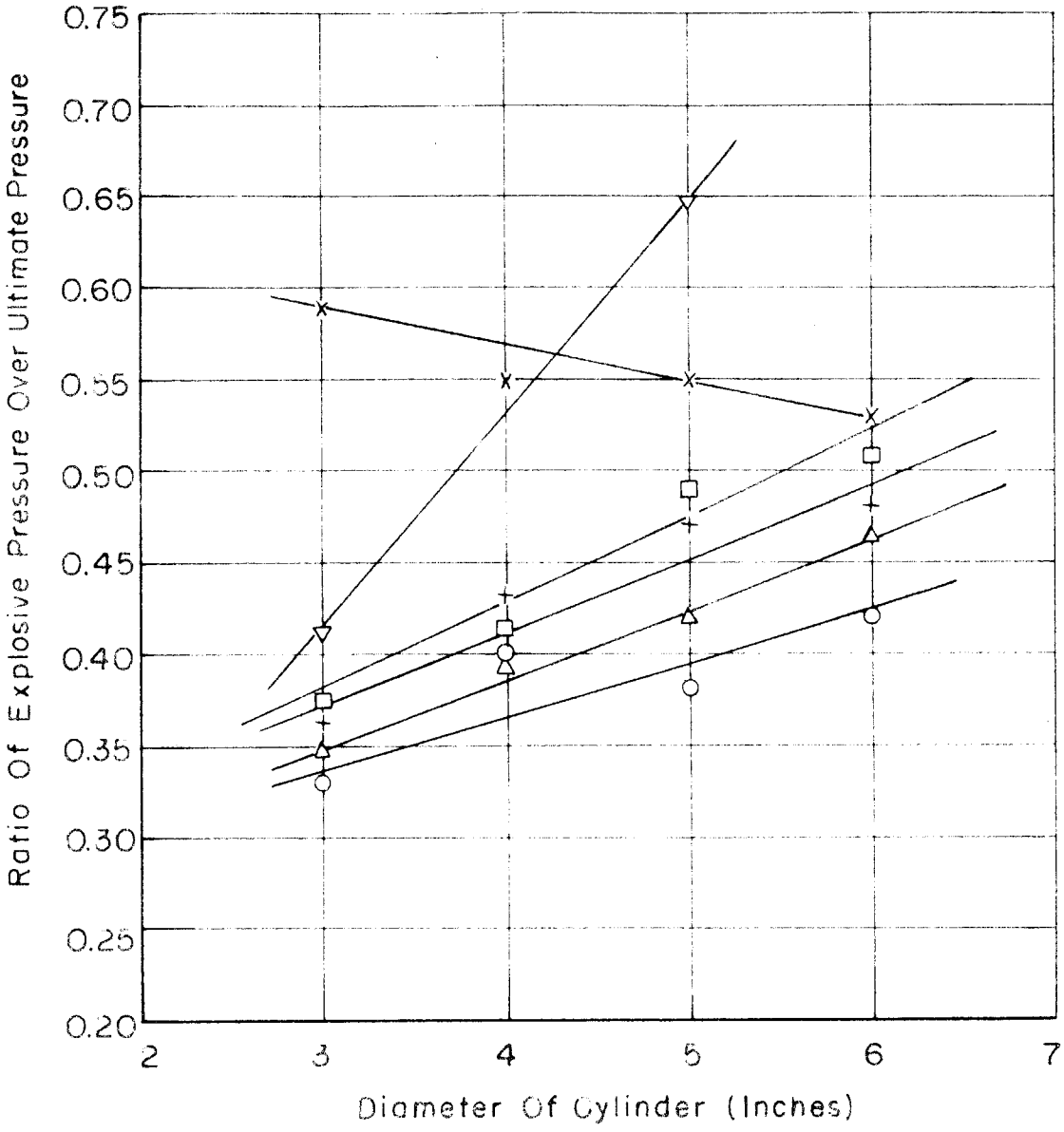

Explosive Level Failure

○	Pellets @ 315 fps 0.001" mat.	High Velocity
△	Darts @ 250 fps 0.001" mat.	
+	Pellets @ 315 fps 0.003" mat.	
□	Darts @ 250 fps 0.003" mat.	
▽	Manual darts @ 40 fps 0.001" mat.	Low Velocity
X	Pellets @ 0 fps 0.001" mat.	

FIG. 9 – NORMALIZED EXPLOSIVE LEVEL

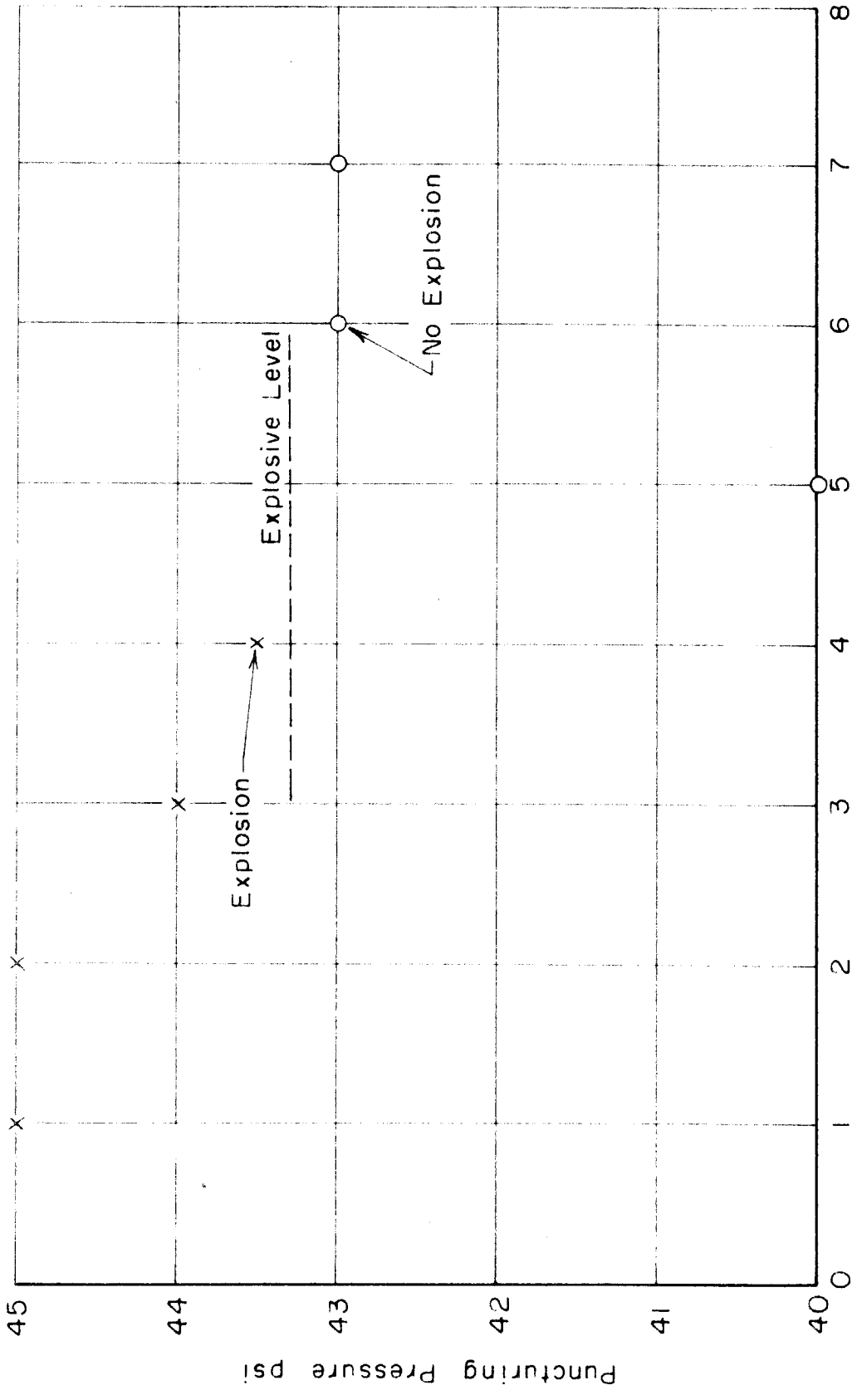

FIG. 10 – DETERMINATION OF EXPLOSIVE LEVEL

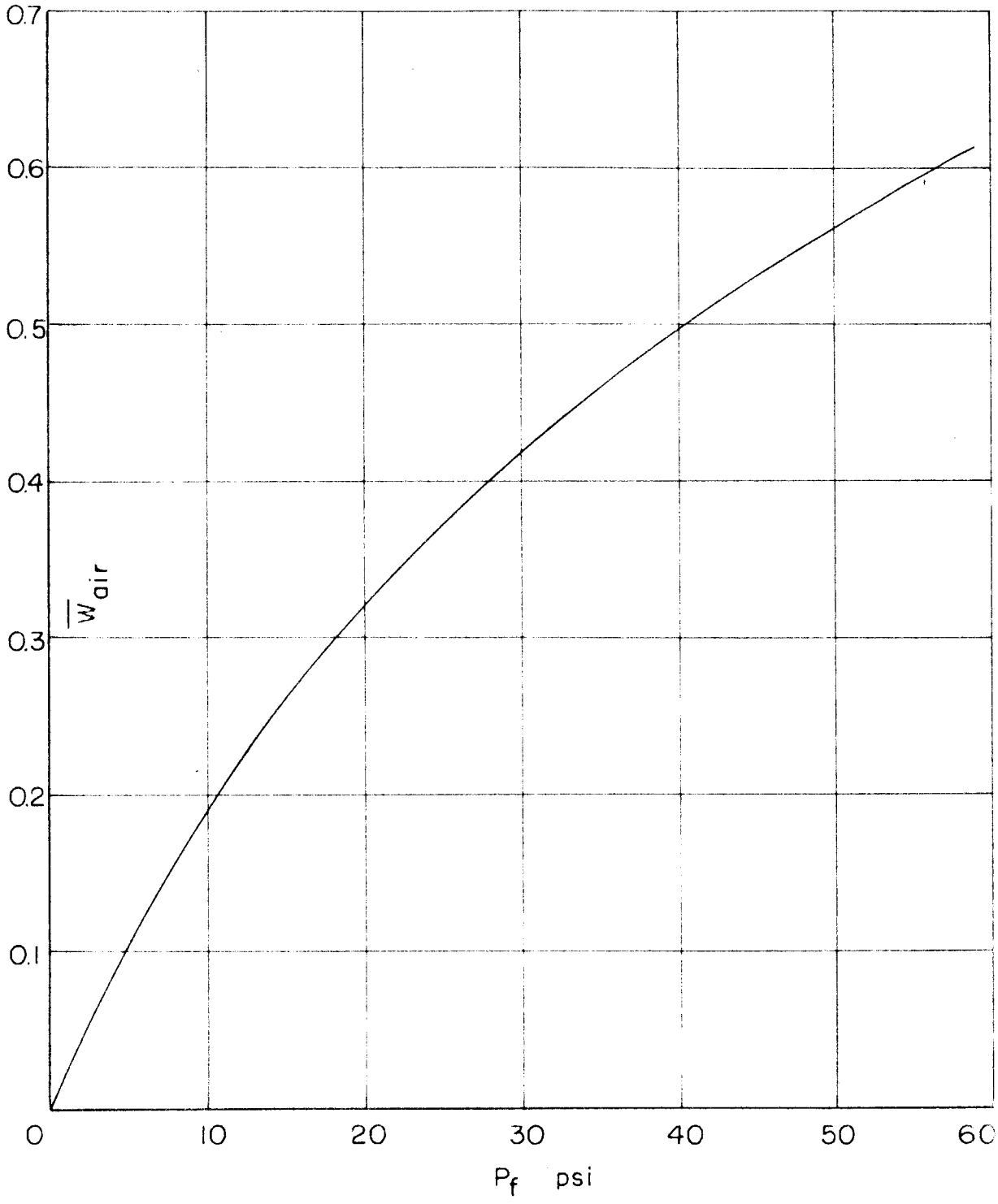

FIG. 11 — NON-DIMENSIONAL AIR ENERGY (REF. 9)

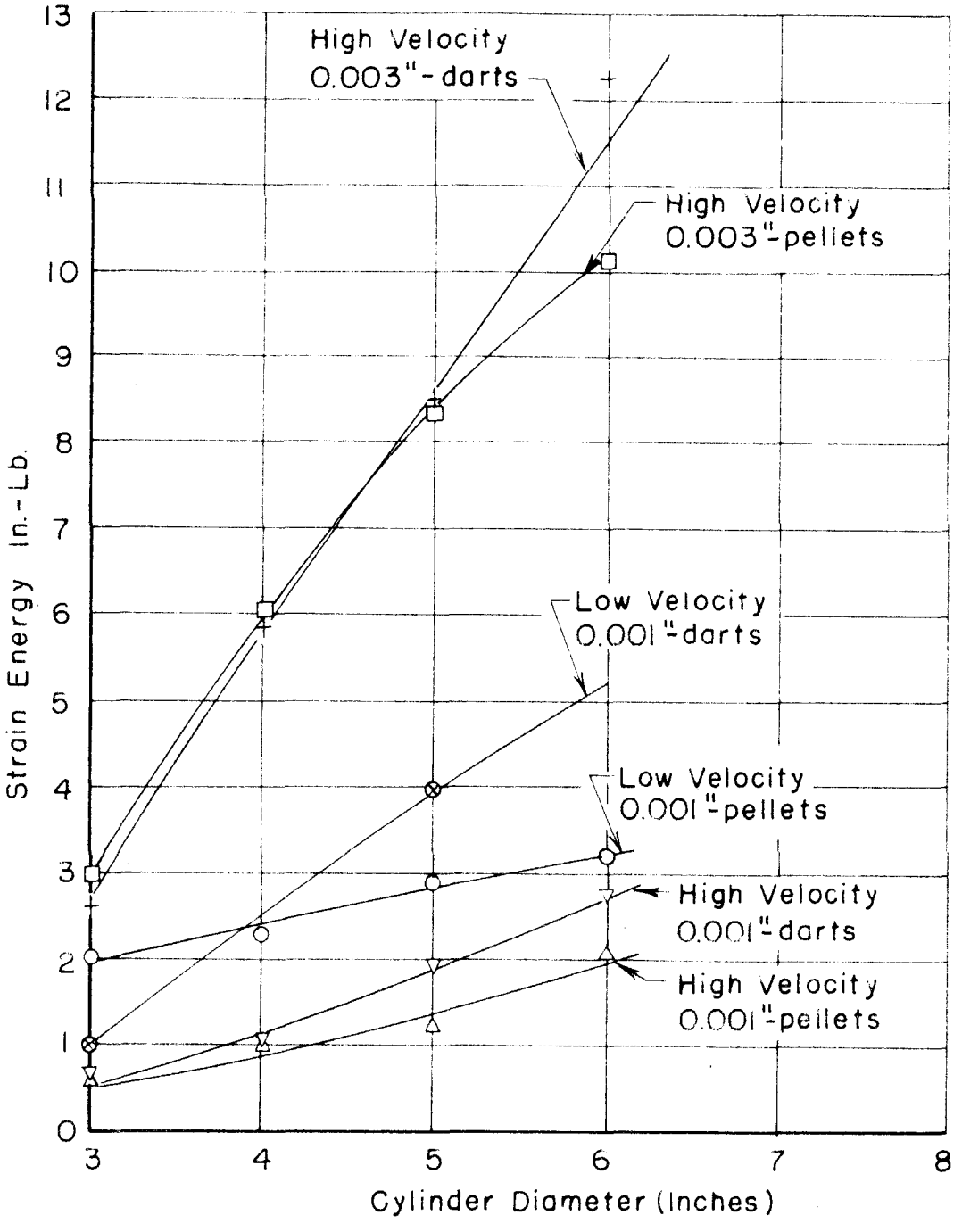

FIG. 12 – STRAIN ENERGY AT EXPLOSIVE LEVEL

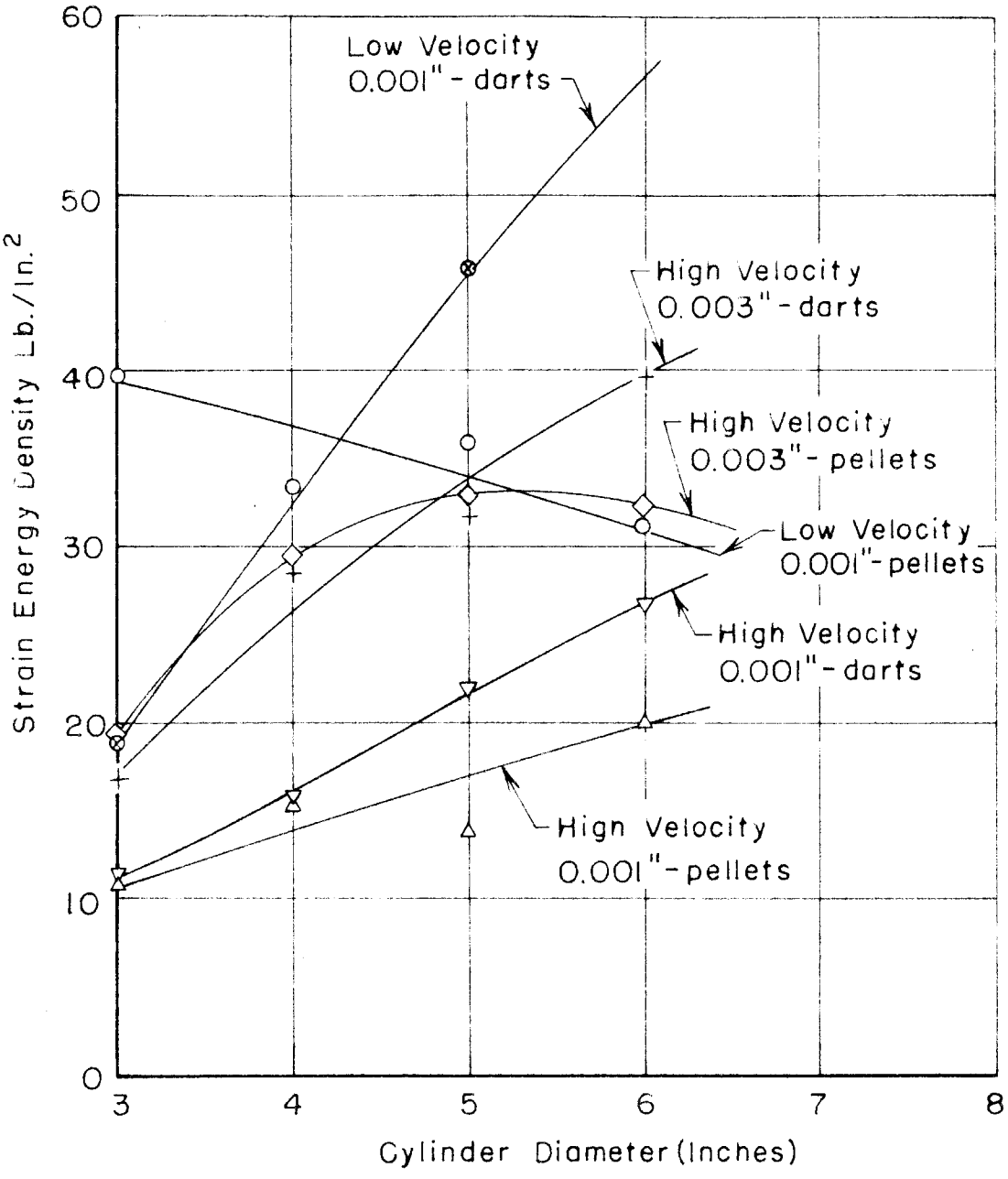

FIG. 13 - STRAIN ENERGY DENSITY AT EXPLOSIVE LEVEL

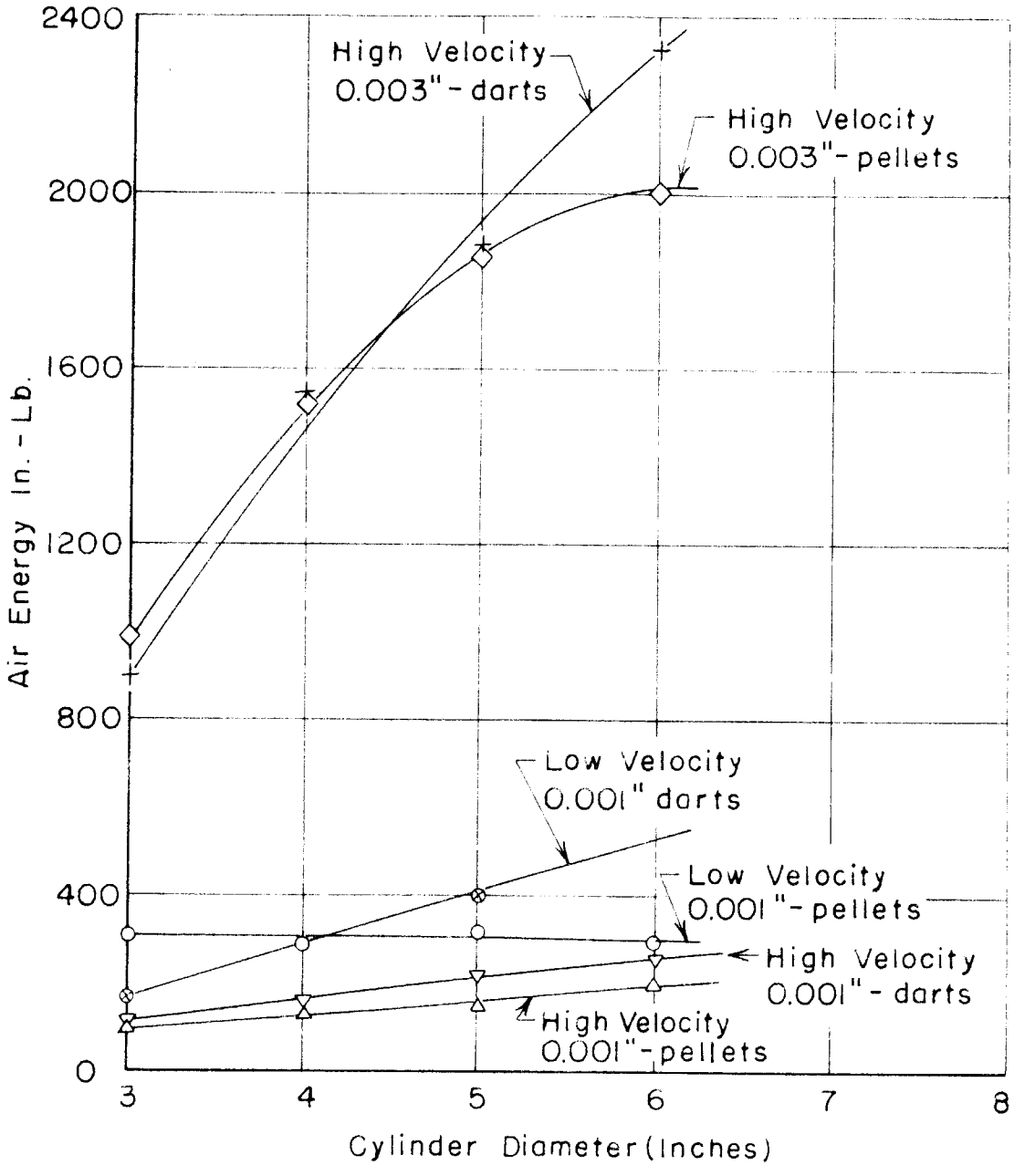

FIG. 14 - AIR ENERGY AT EXPLOSIVE LEVEL

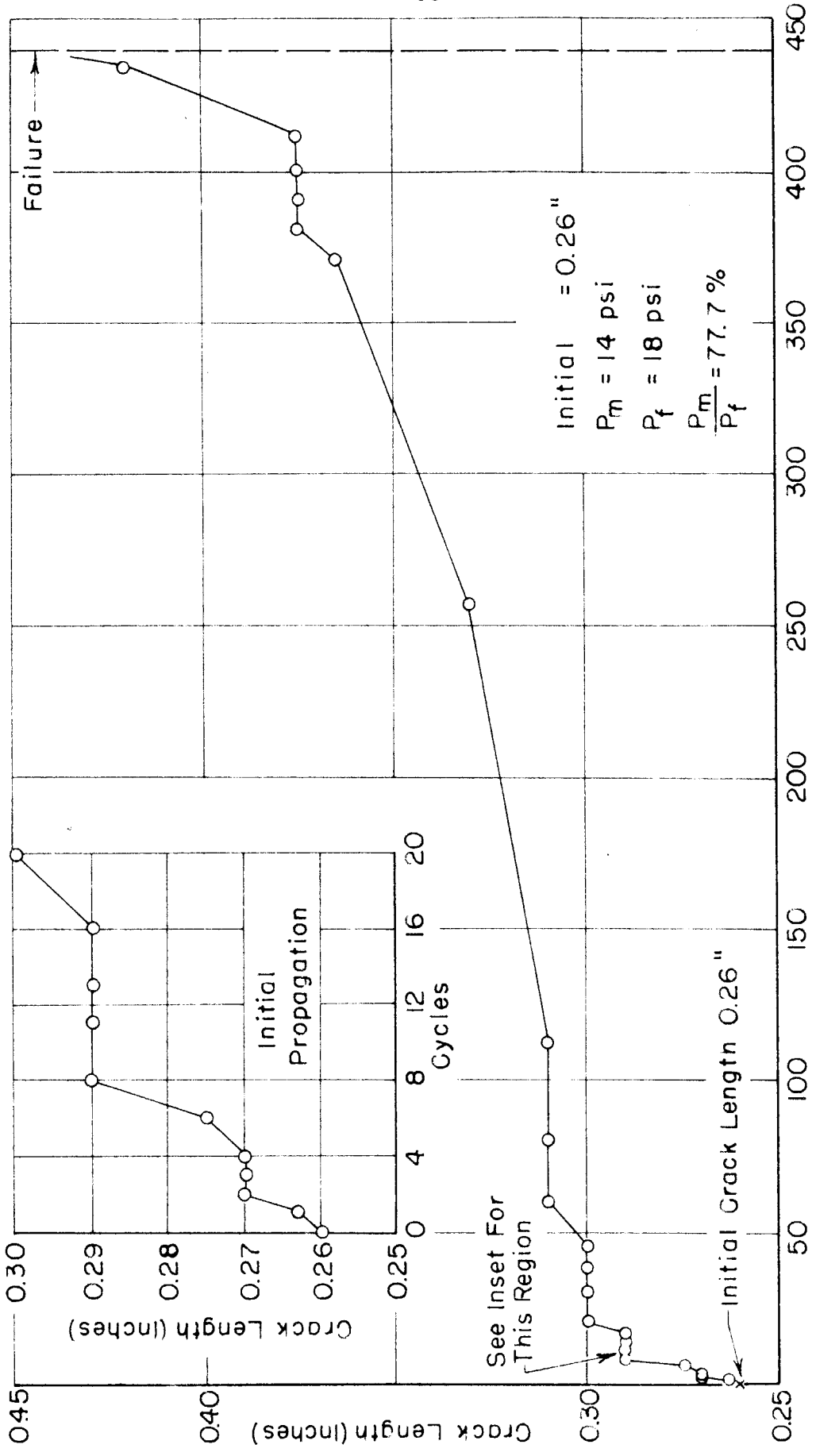

FIG. 15 - CRACK GROWTH FOR 3" - 0.001" CYLINDER UNDER CYCLING PRESSURE

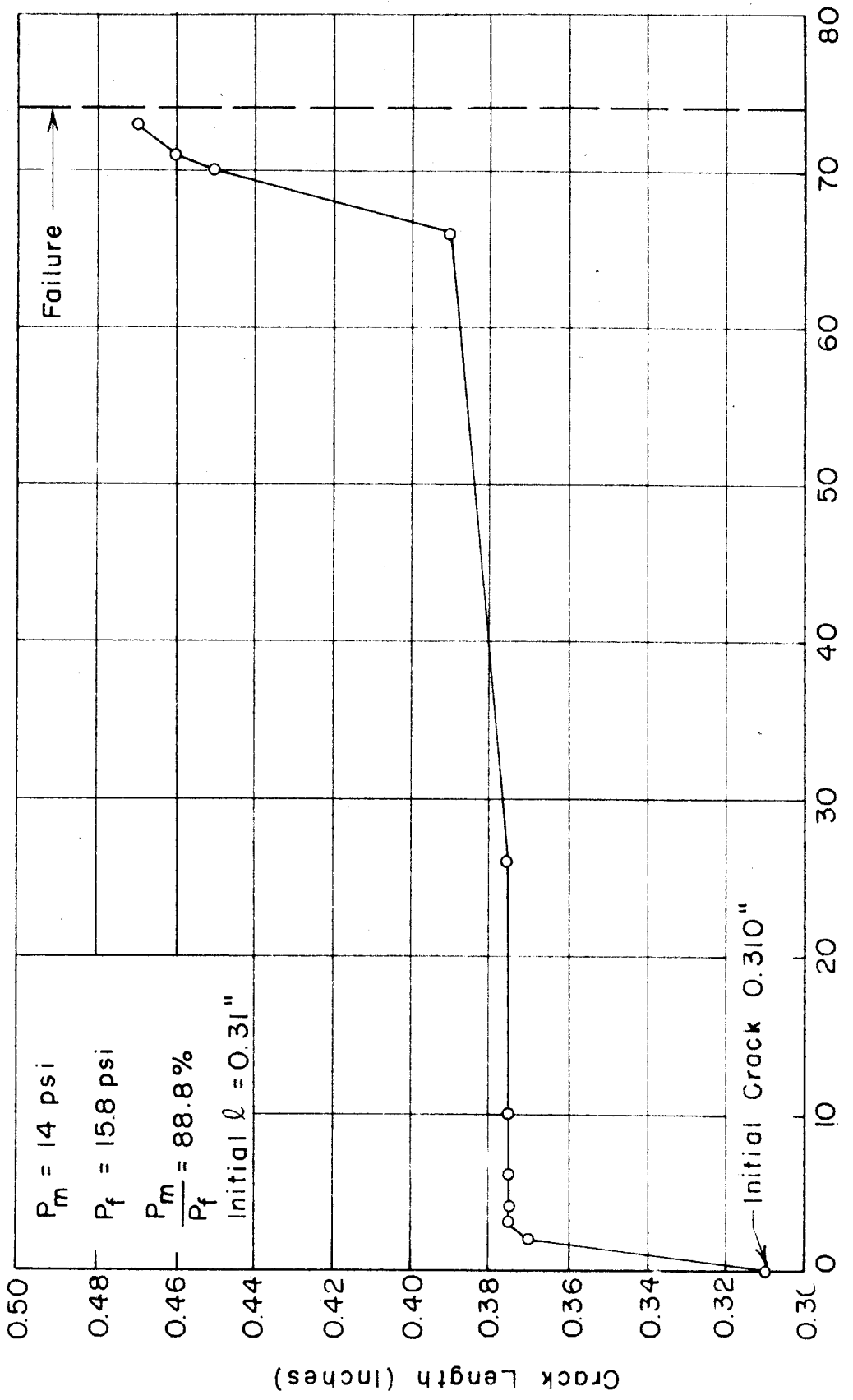

FIG. 16 - CRACK GROWTH FOR 3"-0.001" CYLINDER UNDER CYCLING PRESSURE

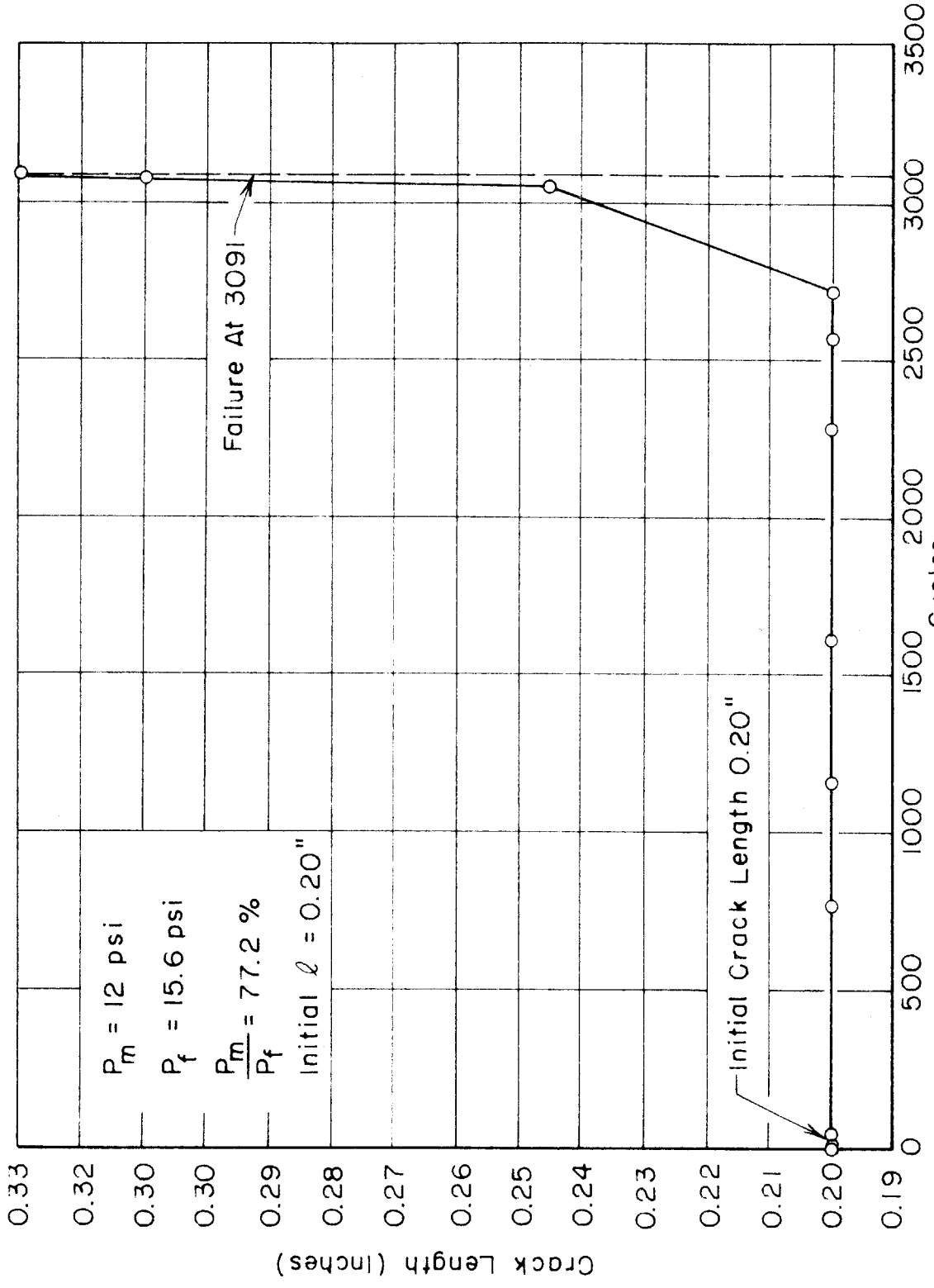

FIG. 17 – CRACK GROWTH FOR 5" – 0.001" CYLINDER UNDER CYCLING PRESSURE

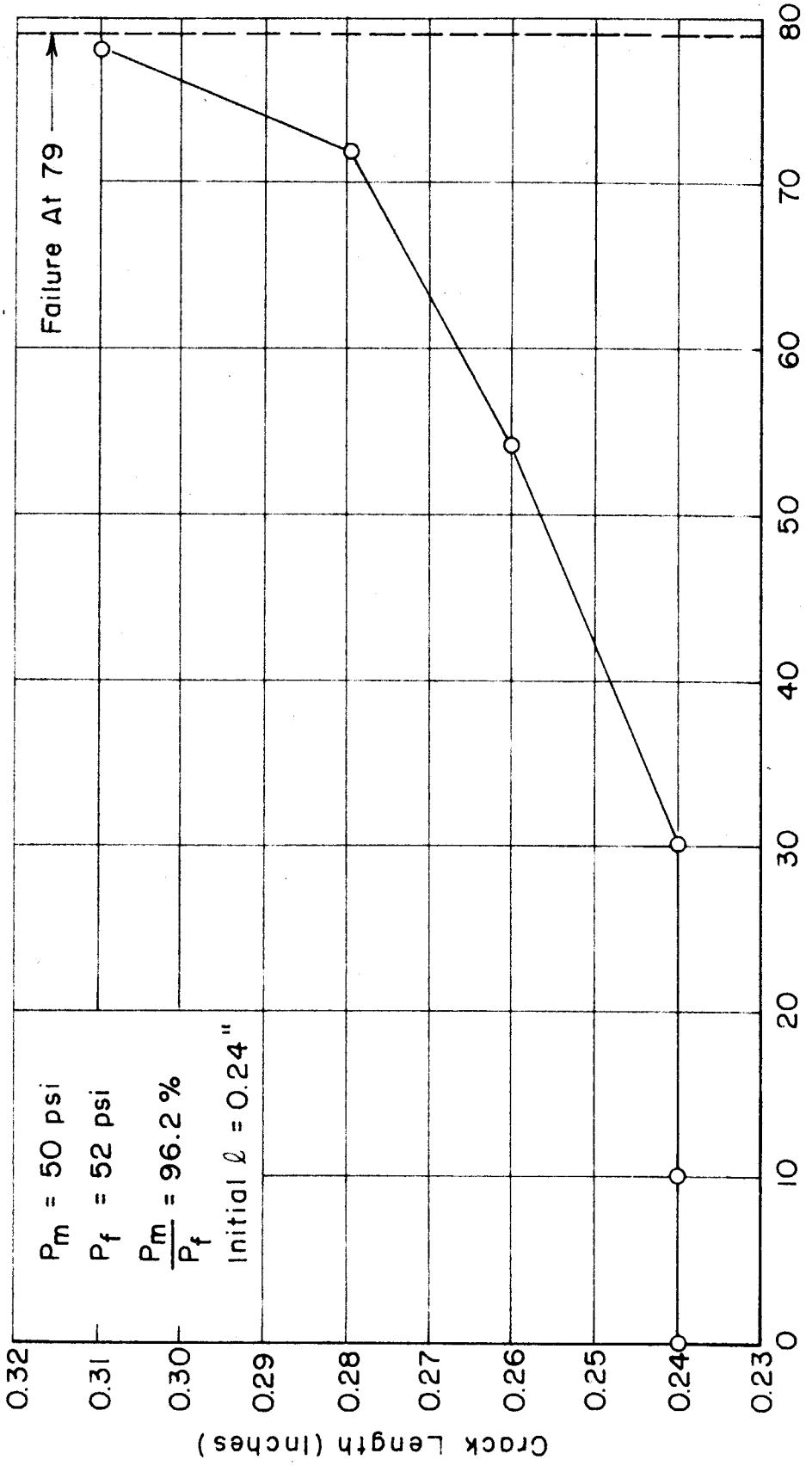

FIG. 18 — CRACK GROWTH FOR 5"-0.003" CYLINDER UNDER CYCLING PRESSURE

TABLE I

CRACK LENGTH VARIATION DATA

FOR 5" - 0.003" CYLINDER

Crack Length l Inches	Failing Pressure P_f p.s.i.	Normalized Pressure $\% \frac{P_f}{P_u}$	Normalized Length $\% \frac{l}{L}$	$\frac{l^2}{td}$
0.000	76.0	100.0	0.00	0.00
0.095	67.6	89.0	1.73	0.60
0.195	59.9	77.5	3.55	2.54
0.230	58.0	76.4	4.18	3.53
0.250	51.0	67.1	4.54	4.16
0.250	54.0	71.1	4.54	4.16
0.250	52.0	68.4	4.54	4.16
0.295	49.6	65.4	5.37	5.81

Ultimate Failing Pressure $P_u = 76.0$ p.s.i.

TABLE II

CRACK LENGTH VARIATION DATA

FOR 5" - 0.001" CYLINDER

Crack Length l Inches	Failing Pressure P_f p.s.i.	Normalized Pressure $\% \frac{P_f}{P_u}$	Normalized Length $\% \frac{l}{L}$	$\frac{l^2}{td}$
0.000	21.5	100.0	0.00	0.00
0.063	19.2	89.2	1.14	0.78
0.063	18.5	86.0	1.14	0.78
0.125	16.0	74.4	2.27	3.12
0.187	14.9	69.8	3.40	7.00
0.187	15.5	72.0	3.40	7.00
0.200	14.0	62.2	3.64	8.00
0.250	12.9	60.0	4.55	12.50
0.250	12.1	56.3	4.55	12.50
0.300	11.0	51.1	5.46	18.00
0.312	10.5	48.9	5.68	19.45
0.312	10.8	50.2	5.68	19.45

Ultimate Failing Pressure $P_u = 21.5$ p.s.i.

TABLE III

CRACK LENGTH VARIATION DATA

FOR 3" - 0.001" CYLINDER

Crack Length l Inches	Failing Pressure P_f p.s.i.	Normalized Pressure $\% \frac{P_f}{P_u}$	Normalized Length $\% \frac{l}{L}$	$\frac{l^2}{td}$
0.000	38.5	100.0	0.00	0.00
0.000	38.0	100.0	0.00	0.00
0.000	38.5	100.0	0.00	0.00
0.060	33.8	88.4	1.09	1.20
0.080	30.4	79.5	1.46	2.13
0.130	24.8	64.9	2.36	5.63
0.200	20.1	52.5	3.64	13.33
0.200	20.0	52.3	3.64	13.33
0.250	17.0	44.5	4.55	20.80
0.250	17.2	45.0	4.55	20.80
0.260	18.0	47.0	4.72	22.50
0.300	15.8	41.4	5.45	30.00
0.300	14.5	37.9	5.45	30.00
0.350	12.8	33.5	6.36	40.80
0.420	12.8	33.5	7.64	58.70
0.500	9.5	24.8	9.10	83.40
0.600	8.9	23.3	10.90	120.00
0.700	7.4	19.4	12.73	163.40

Ultimate Failing Pressure $P_u = 38.3$ p.s.i.

TABLE IV

CRACK ROTATION DATA FOR 5" - 0.001" CYLINDER

WITH 0.125" CRACK

Crack Angle Degrees	Failing Pressure P_f p.s.i.	Normalized Pressure $\% \frac{P_f}{P_u}$
0	16.4	76.3
15	17.2	80.0
15	17.2	80.0
30	17.7	82.4
30	17.9	83.3
30	15.9	74.0
45	18.0	83.7
45	18.2	84.7
60	18.3	85.1
60	19.0	88.4
75	20.1	93.5
75	20.0	93.0
90	22.0	100.0
90	21.0	100.0

Ultimate Failing Pressure $P_u = 21.5$ p.s.i.

TABLE V

CRACK ROTATION DATA FOR 5" - 0.001" CYLINDER

WITH 0.125" CRACK

Crack Angle α Degrees	Failing Pressure P_f p.s.i.	Normalized Pressure $\% \frac{P_f}{P_u}$
22.5	18.5	82.3
22.5	17.7	78.8
45.0	19.7	87.6
45.0	20.3	90.4
67.5	20.0	89.0
67.5	21.6	96.1
90.0	21.7	100.0
90.0	23.8	100.0

Ultimate Failing Pressure $P_u = 22.5$ p.s.i.

TABLE VI

A. EXPLOSIVE LEVELS FOR PELLET RUN

	Low Velocity			High Velocity					
	0.001"			0.001"			0.003"		
Cyl. Dia.	P_e	P_u	$\%\frac{P_e}{P_u}$	P_e	P_u	$\%\frac{P_e}{P_u}$	P_e	P_u	$\%\frac{P_e}{P_u}$
3	22.5	38.0	59.2	12.0	36.0	33.3	47.0	129.0	36.4
4	15.5	28.5	54.4	10.5	26.0	40.4	43.3	98.0	44.2
5	12.5	22.5	55.6	8.0	21.5	37.2	36.8	77.5	47.5
6	10.0	19.0	53.0	8.0	19.0	42.1	30.5	63.9	47.8

B. EXPLOSIVE LEVELS FOR DART RUN

	Low Velocity			High Velocity					
	0.001"			0.001"			0.003"		
Cyl. Dia.	P_e	P_u	$\%\frac{P_e}{P_u}$	P_e	P_u	$\%\frac{P_e}{P_u}$	P_e	P_u	$\%\frac{P_e}{P_u}$
3	15.5	38.0	40.7	12.0	36.0	33.3	44.0	128.0	34.5
4				10.5	26.5	39.5	43.0	104.0	41.4
5	14.5	22.5	64.5	10.3	23.5	43.8	36.8	75.5	48.8
6				9.3	19.6	47.4	33.7	66.5	50.7

All pressures in p.s.i.

TABLE VII

EXAMPLE, DETERMINATION OF EXPLOSIVE LEVEL

High Velocity Pellet Run on 4" - 0.003" Cylinder

Ultimate Failing Pressure P_u = 98 p.s.i.

Pressure p.s.i.	Explosion?	
45.0	Yes	
45.0	Yes	
44.0	Yes	
43.5	Yes	
40.0	No	---Explosive Level P_e = 43.3 p.s.i.
43.0	No	
43.0	No	

Percentage explosive level to ultimate pressure:

$$\frac{P_e}{P_u} \times 100\% = \frac{100 \times 43.3}{98} = 44.2\%$$

TABLE VIII

PROJECTILE HIGH VELOCITIES

Distance from gun muzzle to midpoint of timing strips = 5'

Number of pumps on airgun = 10

Type of Projectile	Distance between Timing Strips feet	Time to Traverse seconds	Velocity fps	Avg. Velocity fps
Flat Nosed Pellets	1.000	0.0026	384	315
	1.000	0.0032	312	
	1.000	0.0031	316	
	1.000	0.0032	312	
	0.833	0.0028	298	
	0.833	0.0031	269	
Darts	0.988	0.0037	264	250
	1.000	0.0040	250	
	1.000	0.0040	250	
	0.833	0.0036	232	

TABLE IX

AIR AND CYLINDER ENERGIES AT EXPLOSIVE LEVEL

AND HIGH VELOCITY PELLET PUNCTURE FOR

0.001" AND 0.003" CYLINDERS

(See Appendix II)

Dia. d in.	Explos. Level P_e p.s.i.	$\overline{W}_{air}$ (Fig 11)	$\frac{W_{cyl}}{W_{air}}$	Strain Energy W_{cyl} in-lb	Strain Energy Density $W_{c\ den}$ lb/in^2	Air Energy W_{air} in-lb
0.001" thick cylinders:						
3	12.0	0.223	0.00563	0.585	11.28	104
4	10.5	0.200	0.00733	1.063	15.36	145
5	8.0	0.160	0.00873	1.205	13.93	152
6	8.0	0.160	0.01048	2.080	20.05	198
0.003" thick cylinders:						
3	47.0	0.543	0.00303	2.99	19.22	987
4	43.5	0.520	0.00389	6.08	29.30	1563
5	36.8	0.475	0.00451	8.50	32.80	1885
6	30.5	0.423	0.00503	10.09	32.45	2005

TABLE X

AIR AND CYLINDER ENERGIES AT EXPLOSIVE LEVEL

AND LOW VELOCITY PELLET AND DART PUNCTURE

FOR 0.001" CYLINDERS

(See Appendix II)

Dia. d in.	Explos. Level P_e p.s.i.	$\overline{W}_{air}$ (Fig. 11)	$\frac{W_{cyl}}{W_{air}}$	Strain Energy W_{cyl} in-lb	Strain Energy Density $W_{c\ den}$ lb/in^2	Air Energy W_{air} in-lb
Pellet Puncture:						
3	22.5	0.35	0.00674	2.06	39.7	306
4	15.5	0.27	0.00802	2.31	33.4	288
5	12.5	0.23	0.00948	2.94	35.9	310
6	10.0	0.19	0.01104	3.25	31.3	294
Dart Puncture:						
3	15.5	0.270	0.00601	0.98	18.8	162
5	14.5	0.255	0.00990	3.95	45.7	399

TABLE XI

AIR AND CYLINDER ENERGIES AT EXPLOSIVE LEVEL AND HIGH VELOCITY DART PUNCTURE FOR 0.001" AND 0.003" CYLINDERS

(See Appendix II)

Dia. d in.	Explos. Level P_e p.s.i.	$\overline{W}_{air}$ (Fig. 11)	$\frac{W_{cyl}}{W_{air}}$	Strain Energy W_{cyl} in-lb	Strain Energy Density $W_{c\ den}$ lb/in^2	Air Energy W_{air} in-lb
0.001" thick cylinders:						
3	12.0	0.223	0.00564	0.585	11.28	104
4	10.5	0.200	0.00732	1.063	15.36	145
5	10.3	0.197	0.00910	1.977	22.90	217
6	9.3	0.180	0.01076	2.783	26.85	259
0.003" thick cylinders:						
3	44.0	0.525	0.00292	2.62	16.8	898
4	43.0	0.517	0.00386	5.94	28.6	1538
5	36.8	0.472	0.00453	8.50	32.8	1875
6	33.7	0.447	0.00526	12.30	39.5	2330

TABLE XII

PRESSURE CYCLING DATA FOR 3"-0.001" CYLINDER

P_m = 14 p.s.i., Initial l = 0.260 in., P_f = 18 p.s.i.,

P_m/P_f = 77.7 °/o

No. Cycles	Crack Length l in.	No. Cycles	Crack Length l in.
0	0.260	45	0.300
1	0.263	60	0.310
2	0.270	80	0.310
3	0.270	112	0.310
4	0.270	257	0.330
6	0.275	371	0.365
8	0.290	381	0.375
11	0.290	391	0.375
13	0.290	401	0.375
16	0.290	411	0.375
20	0.300	434	0.420
30	0.300	440	broke
38	0.300		

TABLE XIII

PRESSURE CYCLING DATA FOR 3"-0.001" CYLINDER

P_m = 14 p.s.i., Initial l = 0.310 in., P_f = 15.8 p.s.i.,

P_m/P_f = 88.8 °/o

No. Cycles	Crack Length l in.
0	0.310
2	0.370
3	0.375
4	0.375
6	0.375
10	0.375
26	0.375
66	0.390
70	0.450
71	0.460
73	0.470
74	Broke

TABLE XIV

PRESSURE CYCLING DATA FOR 5" - 0.001" CYLINDER

P_m = 12 p.s.i., Initial l = 0.200 in., P_f = 15.6 p.s.i.,

P_m/P_f = 77.2°/o

No. cycles	Crack length l in.
0	0.200
5	0.200
765	0.200
1165	0.200
1609	0.200
2281	0.200
2671	0.200
2821	0.200
3049	0.250
3069	0.310
3081	0.330
3091	Broke

TABLE XV

PRESSURE CYCLING DATA FOR 5" - 0.003" CYLINDER

P_m = 50 p.s.i., Initial l = 0.24 in., P_f = 52 p.s.i.,

P_m/P_f = 96.2%

No. cycles	Crack Length l in.
0	0.24
10	0.24
30	0.24
54	0.26
72	0.28
78	0.31
79	Broke

TABLE XVI

MEDIA COMPARISON DATA FOR STATIC FAILURE

WITH 0.125" INITIAL CRACK

$\frac{d}{t}$	dia d in.	th t in. $\times 10^{-3}$	fail. press. P_f p.s.i. water	fail. press. P_f p.s.i. air	avg. failing press. p.s.i. water	avg. failing press. p.s.i. air	avg. failing stress p.s.i. water	avg. failing stress p.s.i. air
750	3	4	190.0	172.0				
750	3	4	160.0	148.0	178.3	167.0	66,780	62,700
750	3	4	185.0	181.0				
1,000	3	3	125.0	112.0				
1,000	3	3	105.0	123.0	118.3	121.0	59,200	60,500
1,000	3	3	125.0	128.0				
1,000	4	4	125.0	110.0				
1,000	4	4	120.0	117.0	123.3	115.6	61,600	57,800
1,000	4	4	125.0	120.0				
1,500	3	2	65.0	65.0				
1,500	3	2	63.0	64.0	64.3	61.7	48,200	46,300
1,500	3	2	65.0	56.0				
1,500	6	4	97.0	95.0				
1,500	6	4	63.0	90.0				
1,500	6	4	92.5		82.6	93.0	55,070	62,000
1,500	6	4	89.0					
1,500	6	4	91.0					
2,000	4	2	48.0	48.5				
2,000	4	2	49.5	52.0	49.3	51.5	49,300	51,500
2,000	4	2	50.5	54.0				

TABLE XVI (Cont'd)

MEDIA COMPARISON DATA FOR STATIC FAILURE

WITH 0.125" INITIAL CRACK

$\frac{d}{t}$	dia. d in.	th t in. $\times 10^3$	fail. press. P_f p.s.i.		avg. failing press. p.s.i.		avg. failing stress p.s.i.	
			water	air	water	air	water	air
2,000	6	3	62.0	64.5				
2,000	6	3	64.0	64.0	66.3	65.2	66,300	65,200
2,000	6	3	73.0	67.0				
2,500	5	2	37.5	35.0				
2,500	5	2	38.0	32.5	38.0	34.2	47,500	42,750
2,500	5	2	38.5	35.0				
3,000	3	1	27.5	24.0				
3,000	3	1	26.5	29.0	26.0	28.0	39,000	42,000
3,000	3	1	23.0	21.0				
3,000	3	1	27.0					
3,000	6	2	31.0	33.0				
3,000	6	2	31.0	30.5	33.7	32.2	50,600	48,300
3,000	6	2	36.0	33.0				
5,000	5	1	17.0	16.5				
5,000	5	1	19.0	17.5	16.5	17.3	41,250	43,250
5,000	5	1	13.5	18.0				
6,000	6	1	17.0	12.0				
6,000	6	1	15.5	16.0	16.2	14.5	48,600	43,500
6,000	6	1	16.0	15.5				

APPENDIX I

PRESENTATION OF CYLINDER STRESSES

AND NOTATION USED IN THIS REPORT

Given the following cylinder:

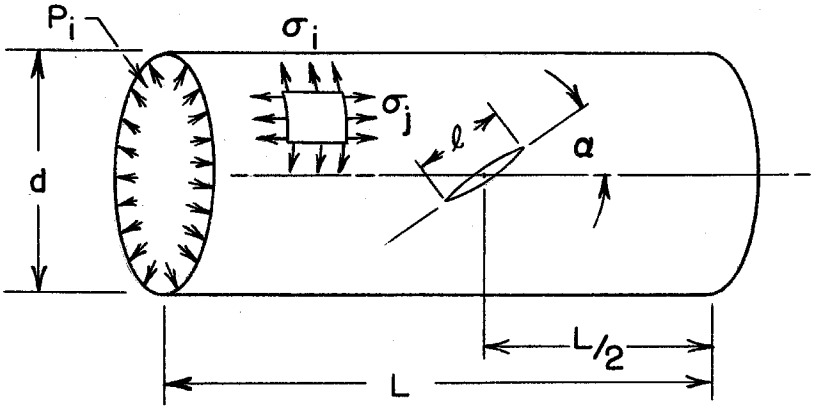

where

d = diameter

t = thickness

L = cylinder length (without ends)

ℓ = crack length

α = crack angle

P_i = internal gage pressure

σ_j = longitudinal stress

σ_i = hoop stress

σ_f = failing hoop stress (with a crack)

σ_e = hoop stress at explosive level (above which explosive failure occurs from penetration)

σ_u = ultimate hoop stress (without a crack)

all lengths are in inches,

all pressures and stresses in p. s. i.

Hoop and longitudinal stresses are derived from equilibrium of forces within the cylinder:

$$\sigma_i = \frac{Pd}{2t}, \qquad \sigma_j = \frac{Pd}{4t}$$

It then follows that, for the same cylinder,

$$\frac{\sigma_i}{\sigma_u} = \frac{\frac{P_i d}{2t}}{\frac{P_u d}{2t}} = \frac{P_i}{P_u}$$

APPENDIX II

ENERGY FORMULA FOR EXPLOSION LEVEL TESTS

(See Reference 9)

The equation derived by Walker for a simple cylinder will be used. Walker derived the equation for a cylinder under internal pressure only with ends infinitely stiff in bending, but which allows the curved walls to expand.

The strain energy of a simple cylinder (due to internal pressure) from equation 20, Reference 9 is:

$$W_{cyl} = \frac{PV(5-4m)T}{4E} = PV \cdot \overline{W}_{cyl}$$

Where: W_{cyl} = Strain energy of side wall, in - lb.

($\overline{W}_{cyl}$ = nondimensional form)

m = Poisson's Ratio

E = Young's Modulus

V = Volume of enclosed space

$= \frac{\pi d^2 L}{4}$

T = Hoop stress = $\sigma_t = \frac{P_i d}{2t}$

Given: $L = 5.5$ in.

$E = 13.6 \times 10^6$ p.s.i. (rolled 1/4 hard brass)

$m = .3$

$$\therefore \quad W_{cyl} = \frac{1.506\ P^2 d^3}{10^7\ t} \text{ in - lb.}$$

Strain energy density:

$$W_{\text{cyl den.}} = \frac{W_{\text{cyl}}}{V_{\text{cyl}}}$$

$$= \frac{W_{\text{cyl}}}{\pi L d t}$$

$$\therefore \quad W_{\text{cyl den.}} = \frac{W_{\text{cyl}}}{5.5 \pi d t} \quad \text{lb/in}^2$$

Available (destructive) air energy will be:

$$W_{\text{air}} = \frac{W_{\text{cyl}}}{\frac{\overline{W}_{\text{cyl}}}{\overline{W}_{\text{air}}}}$$

Where $$\frac{W_{\text{cyl}}}{W_{\text{air}}} = \frac{\overline{W}_{\text{cyl}}}{\overline{W}_{\text{air}}}$$

$$= \frac{(5-4m)T}{4E\ \overline{W}_{\text{air}}}$$

$$= \frac{Pd}{28.65 \times 10^6 t\ \overline{W}_{\text{air}}}$$

$$\therefore \quad W_{\text{air}} = \frac{W_{\text{cyl}}}{\frac{Pd}{28.65 \times 10^6 t\ \overline{W}_{\text{air}}}} \quad \text{in-lb}$$

Where $\overline{W}_{\text{air}}$ is obtained from Fig. 11, knowing P.

Hence P, d, t, and L are necessary and sufficient to calculate the air and strain energies. These energies are tabulated in Tables 9, 10 and 11; and are plotted in Figures 13, 14 and 15.

Example:

Compare air energies at high velocity explosive dart level of 3" diameter cylinders 0.001" and 0.003" thick from data of Table 6:

$$\frac{W_{air\ .003}}{W_{air\ .001}} = \frac{\dfrac{W_{cyl\ .003}}{\left(\dfrac{W_c}{W_a}\right)_{.003}}}{\dfrac{W_{cyl\ .001}}{\left(\dfrac{W_c}{W_a}\right)_{.001}}}$$

$$W_{c\ .003} = \frac{1.506 \times 44^2 \times 3^3}{10^7 \times .003} = 2.62 \text{ in - lb.}$$

$$\left(\frac{W_c}{W_a}\right)_{.003} = \frac{44 \times 3}{28.65 \times 10^6 \times .003 \times .525} = .00292$$

$$W_{c\ .001} = \frac{1.506 \times 12^2 \times 3^3}{10^7 \times .001} = .585 \text{ in - lb.}$$

$$\left(\frac{W_c}{W_a}\right)_{.001} = \frac{12 \times 3}{28.65 \times 10^6 \times .001 \times .223} = .00564$$

$$\frac{W_{air\ .003}}{W_{air\ .001}} = \frac{\dfrac{2.62}{.00292}}{\dfrac{.585}{.00564}} = \frac{898}{104} = 8.65$$

Example:

Compare strain energy densities of above cylinders:

$$W_{c_{den.\ .003}} = \frac{2.62}{5.5\pi \times 3 \times .003} = 16.8 \frac{lb}{in^2}$$

$$W_{c_{den.\ .001}} = \frac{.585}{5.5\pi \times 3 \times .001} = 11.3 \frac{lb}{in^2}$$

$$\therefore \quad \frac{W_{den.\ .003}}{W_{den.\ .001}} = 1.49$$

APPENDIX III

PROPOSED DETERMINATION OF EFFECTIVE AXIAL CRACK LENGTH OF ROTATED CRACKS

From tests, one can obtain a family of failing pressure-crack angle curves for increasing crack lengths:

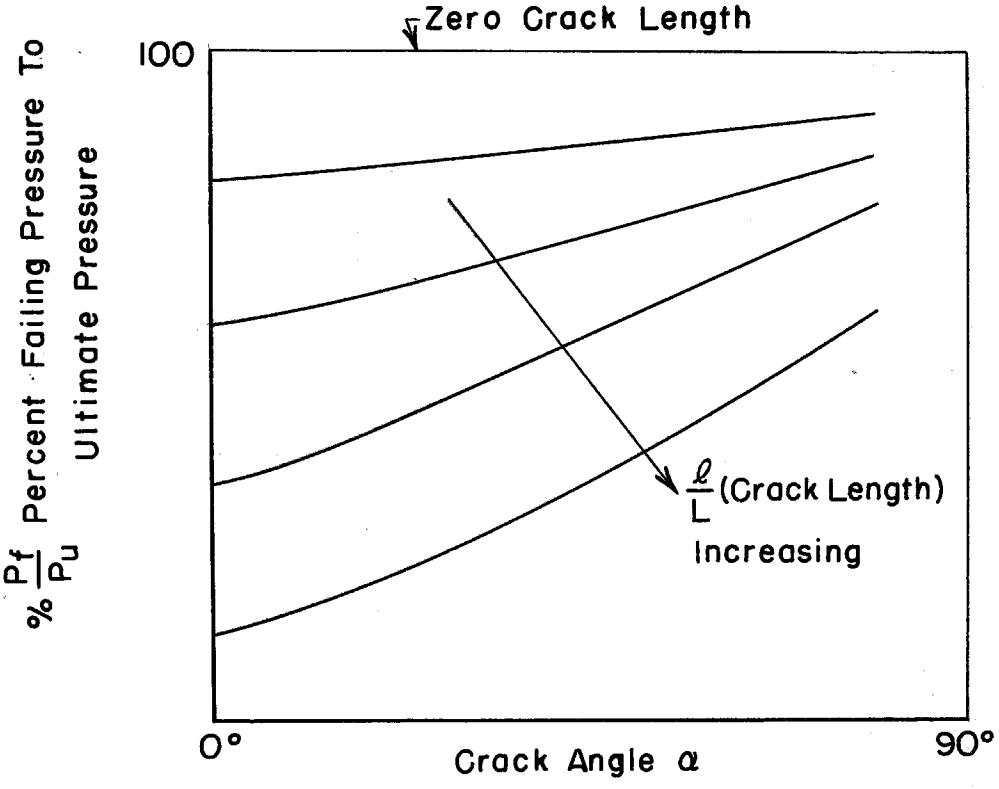

Cross plotting above graph, one obtains crack length-crack angle curves at various failing pressures:

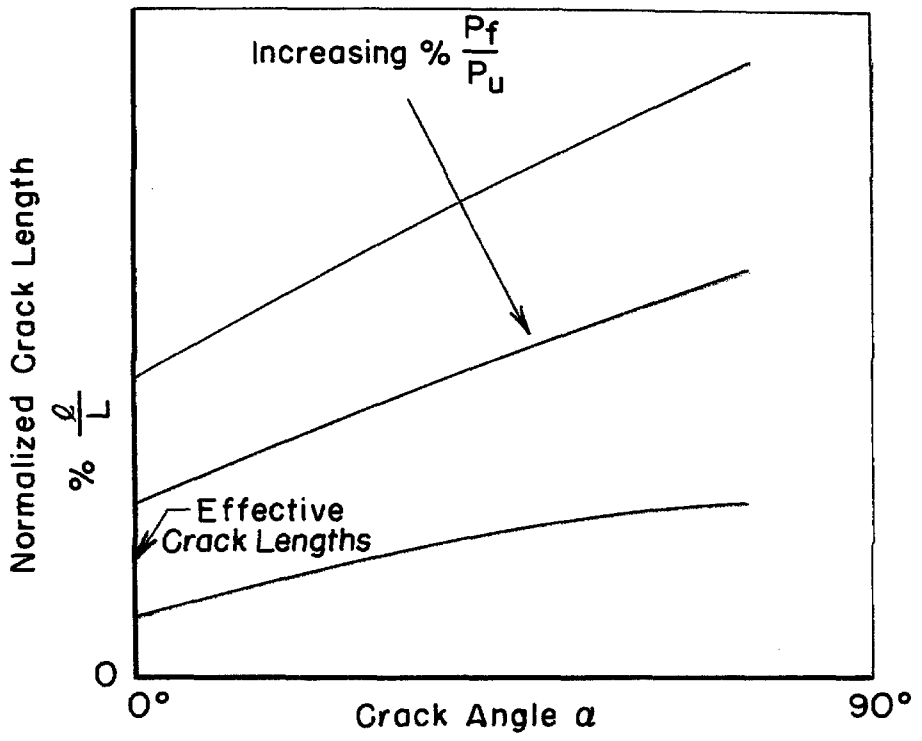

The y-intercepts of the constant failing pressure lines are "effective" crack lengths of various crack length-crack angle combinations.

APPENDIX IV

KINETIC ENERGIES OF PROJECTILES USED IN TEST

Pellets:

Average mass of pellets* = 0.000632 slugs

Average velocity = 315 fps

Kinetic energy = $(1/2)(.000632)(315)^2$ = 31.4 ft - lbs.

Darts:

Average mass of darts* = 0.000992 slugs

Average velocity = 250 fps

Kinetic energy = 31.0 ft - lbs.

*Average of 20 pellets or darts.